HOKKAIDO UNIVERSITY

Title	Fabrication of Tough Hydrogels Composites from Photo-Responsive Polymers to Show Double Network Effect
Author(s)	陶, 真
Degree Grantor	北海道大学
Degree Name	博士(生命科学)
Dissertation Number	甲第13945号
Issue Date	2020-03-25
DOI	https://doi.org/10.14943/doctoral.k13945
Doc URL	https://hdl.handle.net/2115/78122
Type	doctoral thesis
File Information	TAO_Zhen.pdf

Hokkaido University Collection of Scholarly and Academic Papers : HUSCAP

博士学位論文

Doctoral Dissertation

Fabrication of Tough Hydrogels Composites from Photo-Responsive Polymers to Show Double Network Effect

（光応答性ポリマーを用いた新規高靱性ハイドロゲル複合材料の合成とそのダブルネットワーク効果に関する研究）

By

陶　真

Zhen Tao

Supervisor: Jian Ping Gong

Lab of soft & wet Matter

Transdisciplinary Life Science Course

北海道大学大学院生命科学院

Graduate School of Life Science, Hokkaido University

2020 年 3 月

Contents

Chapter 1 General Introduction 4

1.1 Overview 4

1.2 Outline of this thesis 6

Reference 8

Chapter 2 Background 12

2.1 Tough hydrogel 12

2.2 Double network (DN) hydrogels 13

2.2.1 Toughening mechanism of DN gels 13

2.2.2 Development and application of DN gels 14

2.3 Hydrogel composites 15

2.4 Photo-responsive hydrogels 16

Reference 17

Chapter 3 Supramolecular Interaction Form Tough and Self-Healing Hydrogels 24

3.1 Introduction 24

3.2 Experimental 25

3.2.1 Materials 25

3.2.2 Synthesis of hydrogels 26

3.2.3 Characterization of hydrogels 26

3.3 Results and discussion 27

3.3.1 Effect of the fraction of NBOC (f_{NBOC}) *28*

3.3.2 Effect of total monomer concentration (C_m) *29*

3.3.3 Hysteresis and energy dissipation *29*

3.3.4 Self-recovery *30*

3.4 Conclusion 31

Reference 32

Chapter 4 Fabrication of tough hydrogels composites from photo-responsive polymers to show double network effect 40

4.1 Introduction 40

4.2 Experimental 44

4.2.1 Materials *44*

4.2.2 Synthesis of hydrogels *44*

4.2.3 Characterization of hydrogels *45*

4.3 Results and discussion 47

4.3.1 Contrast of physical properties of hydrogel before and after UV irradiation *47*

4.3.2 Contrast of mechanical properties of hydrogel before and after UV irradiation *48*

4.3.3 The effect of factors of UV irradiation on hydrogel samples properties after UV irradiation *48*

4.3.4 The formation of composite hydrogel *50*

4.3.5 The mechanical properties of composite hydrogel *51*

4.3.6 Hysteresis and energy dissipation of composite hydrogel *55*

4.3.7 Patterned composite hydrogel *56*

4.4 Conclusion 57

Reference 57

Chapter 5 Hydrogel composites based on photo-responsive P(HEA-*co*-NBOC) copolymer 81

5.1 Introduction 81

5.2 Experimental 82

5.2.1 Materials *82*

5.2.2 Synthesis of hydrogels *83*

5.2.3 Characterization of hydrogels *83*

5.3 Results and discussion 85

5.3.1 before UV irradiation *85*

5.3.2 After UV irradiation *87*

5.4 Conclusion 89

Reference 90

Chapter 6 Conclusion 102

List of Publications 104

Publications in Scientific Conferences 105

Acknowledge 106

Chapter 1

General Introduction

1.1 Overview

Hydrogels reinforced with rigid skeleton, could exhibit combined characteristics of every component, which remarkably improve the properties and versatile the application of hydrogel[1-4]. However, it still remains to be difficult to develop hydrogel composites performing synergistically improved mechanical properties which requires the matrix component must possess a higher strength than the rigid skeleton[5-7]. Otherwise, the hydrogel composite will not be capable of sustaining high load before fracture. Therefore, to date, many efforts have been done to product energy-dissipated tough hydrogel as the soft matrix, by introduction of reversible crosslinkers[3, 6].

On the other hand, the interface between the soft and rigid phase presents another great challenge. The interface between heterogeneous phases in composite materials plays an essential role in delivery of force and dissipation of energy, resulting in effective reinforcement on the mechanical properties[8]. While, in general, hydrogel composites are formed by polymerization or crosslinking with distrusted phases such as particles, fibers and layer elements as the reinforcing components[2-4]. The swelling mismatch between soft and rigid phases may lead to surface wrinkle, bulk deformation or even

fracture of materials[9-11]. Another practical strategy is to assemble the rigid surface and hydrogels into hybrids by chemical anchoring or physical adhesion.[12-16], But it restricts multiple registration steps or precise chemical design[17, 18].

In this work, we provide a new strategy that integrating the mechanical strong and photo-responsiveness in one hydrogel by copolymerizing hydrophobic stimuli-responsive monomers (2-nitrobenzyloxycarbonylaminoethyl methacrylate, NBOC) into polymer chains. In the gel network, the NBOC residues play two roles, one is working as physical crosslinkers based on their hydrophobic association, which can dissipate large amount of energy during deformation so that toughen the hydrogels; the other is providing photo-responsiveness to further improve the mechanical strength. Specifically, 2-nitrobenzyl functionalities exhibit photo-labile characteristics under UV irradiation, and the resultant amino groups of 2-aminoethyl methacrylate (AMA), which is transformed from NBOC by self-immolative reaction, will further attack the close-by ester bonds, so that replace the original physical crosslinkers by forming new chemical crosslinks, which further increase the modulus of hydrogel.

Our approach is based on copolymers containing pendent photo-responsive, o-nitro benzyl moieties that allow crosslinking at different spatial location to be tuned by UV irradiation, free of multiple stampings or registration steps. With the control the position of UV irradiation, the NBOC-based hydrogels can be easily reconstructed into hieratical structures with different modulus regions.

Furthermore, the mechanical response of this hydrogel composites mimics that of

double-network (DN) gels[20-24], where the hard layers, P(UM-*co*-AMA), act as the first network, imparting high modulus and breaking to dissipate energy, and the soft layer, P(UM-*co*-NBOC) or P(HEA-co-NBOC), acts as the second network, stretching to maintain global integrity. By the observation and investigation of mechanical properties of this hydrogel composites, the hypothesis for fracture mechanism of DN gels could be proved and demonstrated, which has not been witnessed before.

1.2 Outline of this thesis

The research describes in this thesis follows 3 parts. Firstly, the basic study of physical crosslinked P(UM-co-NBOC) hydrogels were elaborated and the composition of P(UM-co-NBOC) hydrogels were optimized. Then, the photo-triggered hydrogel composites were investigated. The damage process of composite agrees with the DN toughening mechanism. Finally, for the university of this strategy, hydrogel composites based on chemical crosslinked P(UM-co-HEA) hydrogels were studied.

In **chapter 3**, tough hydrogels with photo-response were fabricated by introducing a photo-responsive hydrophobic monomer (2-nitrobenzyloxycarbonylaminoethyl methacrylate, NBOC) into hydrophilic polymer networks. By forming the hydrophobic domain, NBOC enhanced the mechanical strength of resultant hydrogel dramatically. Moreover, the hydrogel exhibits improvements in mechanical properties after UV irradiation by forming new chemical crosslinkers that replace the original physical

crosslinkers.

In **chapter 4**, inspired by the toughening mechanism of double-network (DN) gels, tough hydrogel composites with a sandwich structure were fabricated from photo-responsive polymers. By copolymerization of hydrophilic monomers, 2-ureidoethyl methacrylate (UM), and photo-responsive hydrophobic monomers, (2-nitrobenzyloxycarbonylaminoethyl methacrylate, NBOC) at high concentration, physical hydrogels that are soft and highly stretchable are formed due to the hydrophobic associations of NBOC, serving as dynamic crosslinkers. By UV irradiation, the physical crosslinking switches into chemical crosslinking, and the soft physical hydrogels transform to rigid and less stretchable chemical hydrogels. By UV curing the surface layers of the physical hydrogels, we prepared hydrogels composites having sandwiched structure with two rigid outer layers and a soft inner layer. The molecular-level continuous interfaces and matched swelling ratio between the layers ensure the macro-scale hydrogels composites high strength and toughness with a DN gel effect. The outer layers fracture preferentially at deformation, playing a role as like the 1st network of a DN gel, while the inner layer maintains the integrity, playing a role resemble to the 2nd network. The evolution of the fracture morphology of the rigid layers give useful insight on the internal fracture process of DN gels.

In **chapter 5**, we further prepared chemical crosslinked hydrogel by copolymerization of NBOC with 2-hydroxyethyl acrylate (HEA) monomer, which has no strong physical interactions between HEA monomers, to test the universality of the new strategy that

fabricates tough hydrogel composites by incorporating a photo-responsive hydrophobic residue into the hydrogel network.

Reference

1. Ritchie, R. O., The conflicts between strength and toughness. *Nat Mater* **2011,** *10* (11), 817-22.

2. Huang, T.; Xu, H. G.; Jiao, K. X.; Zhu, L. P.; Brown, H. R.; Wang, H. L., A Novel Hydrogel with High Mechanical Strength: A Macromolecular Microsphere Composite Hydrogel. *Advanced Materials* **2007,** *19* (12), 1622-1626.

3. Huang, Y.; King, D. R.; Sun, T. L.; Nonoyama, T.; Kurokawa, T.; Nakajima, T.; Gong, J. P., Energy-Dissipative Matrices Enable Synergistic Toughening in Fiber Reinforced Soft Composites. *Advanced Functional Materials* **2017,** *27* (9).

4. Cheng, Q.; Li, M.; Jiang, L.; Tang, Z., Bioinspired layered composites based on flattened double-walled carbon nanotubes. *Adv Mater* **2012,** *24* (14), 1838-43.

5. Feng, X.; Ma, Z.; MacArthur, J. V.; Giuffre, C. J.; Bastawros, A. F.; Hong, W., A highly stretchable double-network composite. *Soft Matter* **2016,** *12* (44), 8999-9006.

6. Takahashi, R.; Sun, T. L.; Saruwatari, Y.; Kurokawa, T.; King, D. R.; Gong, J. P., Creating Stiff, Tough, and Functional Hydrogel Composites with Low-Melting-

Point Alloys. *Adv Mater* **2018,** *30* (16), e1706885.

7. Cooper, C. B.; Joshipura, I. D.; Parekh, D. P.; Norkett, J.; Mailen, R.; Miller, V. M.; Genzer, J.; Dickey, M. D., Toughening stretchable fibers via serial fracturing of a metallic core. *Sci Adv* **2019,** *5* (2), eaat4600.

8. Gojny, F. H.; Wichmann, M. H. G.; Fiedler, B.; Bauhofer, W.; Schulte, K., Influence of nano-modification on the mechanical and electrical properties of conventional fibre-reinforced composites. *Composites Part A: Applied Science and Manufacturing* **2005,** *36* (11), 1525-1535.

9. Zhang, X.; Pint, C. L.; Lee, M. H.; Schubert, B. E.; Jamshidi, A.; Takei, K.; Ko, H.; Gillies, A.; Bardhan, R.; Urban, J. J.; Wu, M.; Fearing, R.; Javey, A., Optically- and thermally-responsive programmable materials based on carbon nanotube-hydrogel polymer composites. *Nano Lett* **2011,** *11* (8), 3239-44.

10. Kim, M.; Jung, B.; Park, J. H., Hydrogel swelling as a trigger to release biodegradable polymer microneedles in skin. *Biomaterials* **2012,** *33* (2), 668-78.

11. Tanaka, T.; Sun, S. T.; Hirokawa, Y.; Katayama, S.; Kucera, J.; Hirose, Y.; Amiya, T., Mechanical Instability of Gels at the Phase-Transition. *Nature* **1987,** *325* (6107), 796-798.

12. Sudre, G.; Olanier, L.; Tran, Y.; Hourdet, D.; Creton, C., Reversible adhesion between a hydrogel and a polymer brush. *Soft Matter* **2012,** *8* (31).

13. Keplinger, C.; Sun, J. Y.; Foo, C. C.; Rothemund, P.; Whitesides, G. M.; Suo, Z., Stretchable, transparent, ionic conductors. *Science* **2013,** *341* (6149), 984-7.

14. Sun, J. Y.; Keplinger, C.; Whitesides, G. M.; Suo, Z., Ionic skin. *Adv Mater* **2014,** *26* (45), 7608-14.

15. Yang, C. H.; Chen, B. H.; Lu, J. J.; Yang, J. H.; Zhou, J. X.; Chen, Y. M.; Suo, Z. G., Ionic cable. *Extreme Mechanics Letters* **2015,** *3*, 59-65.

16. Han, L.; Lu, X.; Liu, K.; Wang, K.; Fang, L.; Weng, L. T.; Zhang, H.; Tang, Y.; Ren, F.; Zhao, C.; Sun, G.; Liang, R.; Li, Z., Mussel-Inspired Adhesive and Tough Hydrogel Based on Nanoclay Confined Dopamine Polymerization. *ACS Nano* **2017,** *11* (3), 2561-2574.

17. Yuk, H.; Zhang, T.; Lin, S.; Parada, G. A.; Zhao, X., Tough bonding of hydrogels to diverse non-porous surfaces. *Nat Mater* **2016,** *15* (2), 190-6.

18. Yuk, H.; Zhang, T.; Parada, G. A.; Liu, X.; Zhao, X., Skin-inspired hydrogel-elastomer hybrids with robust interfaces and functional microstructures. *Nat Commun* **2016,** *7*, 12028.

19. Wang, X.; Liu, G.; Hu, J.; Zhang, G.; Liu, S., Concurrent block copolymer polymersome stabilization and bilayer permeabilization by stimuli-regulated "traceless" crosslinking. *Angew Chem Int Ed Engl* **2014,** *53* (12), 3138-42.

20. Gong, J. P.; Katsuyama, Y.; Kurokawa, T.; Osada, Y., Double-Network Hydrogels with Extremely High Mechanical Strength. *Advanced Materials* **2003,** *15* (14), 1155-1158.

21. Na, Y.-H.; Kurokawa, T.; Katsuyama, Y.; Tsukeshiba, H.; Gong, J. P.; Osada, Y.; Okabe, S.; Karino, T.; Shibayama, M., Structural Characteristics of

Double Network Gels with Extremely High Mechanical Strength. *Macromolecules* **2004,** *37* (14), 5370-5374.

22. Na, Y.-H.; Tanaka, Y.; Kawauchi, Y.; Furukawa, H.; Sumiyoshi, T.; Gong, J. P.; Osada, Y., Necking Phenomenon of Double-Network Gels. *Macromolecules* **2006,** *39* (14), 4641-4645.

23. Nakajima, T.; Furukawa, H.; Tanaka, Y.; Kurokawa, T.; Osada, Y.; Gong, J. P., True Chemical Structure of Double Network Hydrogels. *Macromolecules* **2009,** *42* (6), 2184-2189.

24. Huang, M.; Furukawa, H.; Tanaka, Y.; Nakajima, T.; Osada, Y.; Gong, J. P., Importance of Entanglement between First and Second Components in High-Strength Double Network Gels. *Macromolecules* **2007,** *40* (18), 6658-6664.

Chapter 2

Background

2.1 Tough hydrogel

Hydrogel is crosslinked hydrophilic polymer networks with a large amount of water, which are resemble biological soft tissues.[1] Due to its combination both of solid and liquid properties, synthetic polymeric hydrogels are extensively developed and used in industrial, biomedical and environmental areas.[2-5] However, when compared with natural hydrogels, which are tough to support the surrounding components, they tend to be very brittle and soft, which leads to inferior mechanical performances, such as low fracture toughness and low strength, frequently hampering applications and innovations of soft materials.[6]

To date, many efforts have been done to improve the toughness of hydrogels by introducing dissipation energy into hydrogels.[6-9] The mechanism for dissipating mechanical energy could be constructed by fracture of polymer chains[10], reversible crosslinking of polymer chains[7], transformation of domains in polymer chains or crosslinkers[11], and fracture and pullout of fibers or fillers[12]. In addition, high stretchability is another critical property for hydrogels to achieve high fracture energy and toughness[9]. The strategy for maintaining elasticity could be performed by

interpenetration of long-chain networks[10], hybrid physical and chemical crosslinkers[3], high-functionality crosslinkers,[13] networks with long monodisperse polymer chains[14], and meso-/macro-scale composites.[15] Over several years, synthetic hydrogels can now be made much tougher than articular cartilages[7, 10] by combined mechanisms.

2.2 Double network (DN) hydrogels

Despite containing 80 to 90 weight percent (wt %) of water, double-network hydrogels (DN gels) consisting of a rigid strong polyelectrolyte network (1st network) and a flexible neutral polymer network (2nd network), show excellent strength, extensibility, and toughness, comparable to that of rubbers and cartilages.

2.2.1 Toughening mechanism of DN gels

The high toughness of DN gels mainly derive from their special double network structure. The rigid, brittle polyelectrolyte, 1st network serves as a sacrificial bond, while the soft, ductile neural 2nd network serves as hidden length that sustains stress by large extension afterwards.[16] During deformation, the 1st network fractures into fragmentation while the 2nd network maintains the integrity of the whole hydrogel sample, thereby suppressing the scale-up of microcracks induced by the break of the 1st network. As a result, before the second network fracture, an extremely large amount of

energy is dissipated due to the internal fracture of the 1st network by large amounts of microcracks are in co-existence because of the distribution of stress, which dramatically contributes to the toughness and other mechanical properties of DN gels.

2.2.2 Development and application of DN gels

It is noted that to endow the hydrogel with high toughness, the system should satisfy the following condition: the stretchablity and strength of the 1st network are much poorer than those of the 2nd network.[17] DN gels become tough regardless of their chemical constituents if the two networks satisfy the above-mentioned conditions. Therefore, tough BC/gelatin (bacterial cellulose gels, produced by *Acetobacter xylinum*) DN hydrogels constructed completely from natural materials were successfully developed by combining these two kinds of gel in order to compensate for each of their individual weaknesses[18].

Demonstrating that sacrificial bonds and the "double network" concept works on length scales far beyond the molecular scale will open these materials for structural applications. Based on the toughening mechanism of DN gels, hydrogel composites with macro-scale rigid and sacrificial skeleton, such as low melting point alloys[15] or 3D-printed grids used as the 1st network were reported.

Since the DN gels show high toughness and mechanical properties with high water content, it is with great potential to apply DN gels to biomedicine, such as regeneration

medicine. Till now, present studies have demonstrated that the DN gel could act as a promising device to enable cell-free cartilage regeneration with potential applications to various defect sizes.[19]

2.3 Hydrogel composites

Hydrogels reinforced with rigid skeleton, could exhibit combined characteristics of every component, which remarkably improve the properties and versatile the application of hydrogel[8, 12, 20, 21]. However, it still remains to be difficult to develop hydrogel composites performing synergistically improved mechanical properties which requires the matrix component must possess a higher strength than the rigid skeleton[15, 22, 23]. Otherwise, the hydrogel composite will not be capable of sustaining high load before fracture. Therefore, to date, many efforts have been done to product energy-dissipated tough hydrogel as the soft matrix, by introduction of reversible crosslinkers[12, 15].

On the other hand, the interface between the soft and rigid phase presents another great challenge. The interface between heterogeneous phases in composite materials plays an essential role in delivery of force and dissipation of energy, resulting in effective reinforcement on the mechanical properties[24]. While, in general, hydrogel composites are formed by polymerization or crosslinking with distrusted phases such as particles, fibers and layer elements as the reinforcing components[12, 20, 21]. The swelling mismatch

between soft and rigid phases may lead to surface wrinkle, bulk deformation or even fracture of materials[25-27]. Another practical strategy is to assemble the rigid surface and hydrogels into hybrids by chemical anchoring or physical adhesion.[28-32], But it restricts multiple registration steps or precise chemical design[33, 34].

2.4 Photo-responsive hydrogels

To mimic natural hydrogels showing response under external stimulus, synthetic polymers materials performing similar attributes have been widely developed,[35, 36] which could be capable of conformational, physical or chemical changes on receiving an external signal, such as pH[37], temperature[38], light,[39-41] electric and magnetic fields,[42] and specific bioactive molecules and metabolites.[43] Over the past few decades, extensive attention has paid to the stimuli-responsive polymers for a variety of applications, such as switching surfaces and adhesives[39], soft robots[44]and biomedical device.[45, 46]

Among various stimuli-responsiveness, photo-responsiveness is attractive due to the inherent advantages that allows remote manipulation of materials without invasion.[47] Moreover, spatial and temporal control could be achieved by modulation of irradiation parameters, such as light intensity and irradiation time[48, 49].

The photo-responsiveness usually arises from functional groups incorporated in the system by photo-triggered cleavage, addition, exchange and isomerization, which

would lead to different response in these hydrogels, including hydrogel formation or degradation, network contraction or expansion, and chemical modifications in the network.[47]

Reference

1. Gong, J. P., Materials science. Materials both tough and soft. *Science* **2014,** *344* (6180), 161-2.

2. Lee, K. Y.; Mooney, D. J., Hydrogels for Tissue Engineering. *Chemical Reviews* **2001,** *101* (7), 1869-1880.

3. Calvert, P., Hydrogels for Soft Machines. *Advanced Materials* **2009,** *21* (7), 743-756.

4. Kumacheva, E., Hydrogels: The catalytic curtsey. *Nat Mater* **2012,** *11* (8), 665-6.

5. Seliktar, D., Designing cell-compatible hydrogels for biomedical applications. *Science* **2012,** *336* (6085), 1124-8.

6. Zhao, X., Designing toughness and strength for soft materials. *Proc Natl Acad Sci U S A* **2017**.

7. Sun, J. Y.; Zhao, X.; Illeperuma, W. R.; Chaudhuri, O.; Oh, K. H.;

Mooney, D. J.; Vlassak, J. J.; Suo, Z., Highly stretchable and tough hydrogels. *Nature* **2012,** *489* (7414), 133-6.

8. Ritchie, R. O., The conflicts between strength and toughness. *Nat Mater* **2011,** *10* (11), 817-22.

9. Zhao, X., Multi-scale multi-mechanism design of tough hydrogels: building dissipation into stretchy networks. *Soft Matter* **2014,** *10* (5), 672-687.

10. Gong, J. P.; Katsuyama, Y.; Kurokawa, T.; Osada, Y., Double-Network Hydrogels with Extremely High Mechanical Strength. *Advanced Materials* **2003,** *15* (14), 1155-1158.

11. Brown, A. E.; Litvinov, R. I.; Discher, D. E.; Purohit, P. K.; Weisel, J. W., Multiscale mechanics of fibrin polymer: gel stretching with protein unfolding and loss of water. *Science* **2009,** *325* (5941), 741-4.

12. Huang, Y.; King, D. R.; Sun, T. L.; Nonoyama, T.; Kurokawa, T.; Nakajima, T.; Gong, J. P., Energy-Dissipative Matrices Enable Synergistic Toughening in Fiber Reinforced Soft Composites. *Advanced Functional Materials* **2017,** *27* (9).

13. Haque, M. A.; Kurokawa, T.; Kamita, G.; Gong, J. P., Lamellar Bilayers as Reversible Sacrificial Bonds To Toughen Hydrogel: Hysteresis, Self-Recovery, Fatigue Resistance, and Crack Blunting. *Macromolecules* **2011,** *44* (22), 8916-8924.

14. Okumura, Y.; Ito, K., The Polyrotaxane Gel: A Topological Gel by Figure-of-Eight Cross-links. *Advanced Materials* **2001,** *13* (7), 485-487.

15. Takahashi, R.; Sun, T. L.; Saruwatari, Y.; Kurokawa, T.; King, D. R.; Gong, J. P., Creating Stiff, Tough, and Functional Hydrogel Composites with Low-Melting-Point Alloys. *Adv Mater* **2018,** *30* (16), e1706885.

16. Gong, J. P., Why are double network hydrogels so tough? *Soft Matter* **2010,** *6* (12).

17. Nakajima, T.; Sato, H.; Zhao, Y.; Kawahara, S.; Kurokawa, T.; Sugahara, K.; Gong, J. P., A Universal Molecular Stent Method to Toughen any Hydrogels Based on Double Network Concept. *Advanced Functional Materials* **2012,** *22* (21), 4426-4432.

18. Haque, M. A.; Kurokawa, T.; Gong, J. P., Super tough double network hydrogels and their application as biomaterials. *Polymer* **2012,** *53* (9), 1805-1822.

19. Higa, K.; Kitamura, N.; Goto, K.; Kurokawa, T.; Gong, J. P.; Kanaya, F.; Yasuda, K., Effects of osteochondral defect size on cartilage regeneration using a double-network hydrogel. *BMC Musculoskelet Disord* **2017,** *18* (1), 210.

20. Huang, T.; Xu, H. G.; Jiao, K. X.; Zhu, L. P.; Brown, H. R.; Wang, H. L., A Novel Hydrogel with High Mechanical Strength: A Macromolecular Microsphere Composite Hydrogel. *Advanced Materials* **2007,** *19* (12), 1622-1626.

21. Cheng, Q.; Li, M.; Jiang, L.; Tang, Z., Bioinspired layered composites based on flattened double-walled carbon nanotubes. *Adv Mater* **2012,** *24* (14), 1838-43.

22. Feng, X.; Ma, Z.; MacArthur, J. V.; Giuffre, C. J.; Bastawros, A. F.; Hong, W., A highly stretchable double-network composite. *Soft Matter* **2016,** *12* (44),

8999-9006.

23. Cooper, C. B.; Joshipura, I. D.; Parekh, D. P.; Norkett, J.; Mailen, R.; Miller, V. M.; Genzer, J.; Dickey, M. D., Toughening stretchable fibers via serial fracturing of a metallic core. *Sci Adv* **2019,** *5* (2), eaat4600.

24. Gojny, F. H.; Wichmann, M. H. G.; Fiedler, B.; Bauhofer, W.; Schulte, K., Influence of nano-modification on the mechanical and electrical properties of conventional fibre-reinforced composites. *Composites Part A: Applied Science and Manufacturing* **2005,** *36* (11), 1525-1535.

25. Zhang, X.; Pint, C. L.; Lee, M. H.; Schubert, B. E.; Jamshidi, A.; Takei, K.; Ko, H.; Gillies, A.; Bardhan, R.; Urban, J. J.; Wu, M.; Fearing, R.; Javey, A., Optically- and thermally-responsive programmable materials based on carbon nanotube-hydrogel polymer composites. *Nano Lett* **2011,** *11* (8), 3239-44.

26. Kim, M.; Jung, B.; Park, J. H., Hydrogel swelling as a trigger to release biodegradable polymer microneedles in skin. *Biomaterials* **2012,** *33* (2), 668-78.

27. Tanaka, T.; Sun, S. T.; Hirokawa, Y.; Katayama, S.; Kucera, J.; Hirose, Y.; Amiya, T., Mechanical Instability of Gels at the Phase-Transition. *Nature* **1987,** *325* (6107), 796-798.

28. Sudre, G.; Olanier, L.; Tran, Y.; Hourdet, D.; Creton, C., Reversible adhesion between a hydrogel and a polymer brush. *Soft Matter* **2012,** *8* (31).

29. Keplinger, C.; Sun, J. Y.; Foo, C. C.; Rothemund, P.; Whitesides, G. M.; Suo, Z., Stretchable, transparent, ionic conductors. *Science* **2013,** *341* (6149), 984-

7.

30. Sun, J. Y.; Keplinger, C.; Whitesides, G. M.; Suo, Z., Ionic skin. *Adv Mater* **2014,** *26* (45), 7608-14.

31. Yang, C. H.; Chen, B. H.; Lu, J. J.; Yang, J. H.; Zhou, J. X.; Chen, Y. M.; Suo, Z. G., Ionic cable. *Extreme Mechanics Letters* **2015,** *3*, 59-65.

32. Han, L.; Lu, X.; Liu, K.; Wang, K.; Fang, L.; Weng, L. T.; Zhang, H.; Tang, Y.; Ren, F.; Zhao, C.; Sun, G.; Liang, R.; Li, Z., Mussel-Inspired Adhesive and Tough Hydrogel Based on Nanoclay Confined Dopamine Polymerization. *ACS Nano* **2017,** *11* (3), 2561-2574.

33. Yuk, H.; Zhang, T.; Lin, S.; Parada, G. A.; Zhao, X., Tough bonding of hydrogels to diverse non-porous surfaces. *Nat Mater* **2016,** *15* (2), 190-6.

34. Yuk, H.; Zhang, T.; Parada, G. A.; Liu, X.; Zhao, X., Skin-inspired hydrogel-elastomer hybrids with robust interfaces and functional microstructures. *Nat Commun* **2016,** *7*, 12028.

35. Stuart, M. A.; Huck, W. T.; Genzer, J.; Muller, M.; Ober, C.; Stamm, M.; Sukhorukov, G. B.; Szleifer, I.; Tsukruk, V. V.; Urban, M.; Winnik, F.; Zauscher, S.; Luzinov, I.; Minko, S., Emerging applications of stimuli-responsive polymer materials. *Nat Mater* **2010,** *9* (2), 101-13.

36. Xia, L. W.; Xie, R.; Ju, X. J.; Wang, W.; Chen, Q.; Chu, L. Y., Nano-structured smart hydrogels with rapid response and high elasticity. *Nat Commun* **2013,** *4*, 2226.

37. Kureha, T.; Aoki, D.; Hiroshige, S.; Iijima, K.; Aoki, D.; Takata, T.; Suzuki, D., Decoupled Thermo- and pH-Responsive Hydrogel Microspheres Cross-Linked by Rotaxane Networks. *Angew Chem Int Ed Engl* **2017,** *56* (48), 15393-15396.

38. Miyata, T.; Asami, N.; Uragami, T., A reversibly antigen-responsive hydrogel. *Nature* **1999,** *399* (6738), 766-9.

39. Gao, Y.; Wu, K.; Suo, Z., Photodetachable Adhesion. *Adv Mater* **2019,** *31* (6), e1806948.

40. Huang, X.; Sun, Y.; Soh, S., Stimuli-Responsive Surfaces for Tunable and Reversible Control of Wettability. *Adv Mater* **2015,** *27* (27), 4062-8.

41. Tao, Z.; Peng, K.; Fan, Y. J.; Liu, Y. F.; Yang, H. Y., Multi-stimuli responsive supramolecular hydrogels based on Fe3+ and diblock copolymer micelle complexation. *Polym Chem-Uk* **2016,** *7* (7), 1405-1412.

42. Palleau, E.; Morales, D.; Dickey, M. D.; Velev, O. D., Reversible patterning and actuation of hydrogels by electrically assisted ionoprinting. *Nat Commun* **2013,** *4*, 2257.

43. Kim, J.; Nayak, S.; Lyon, L. A., Bioresponsive hydrogel microlenses. *J Am Chem Soc* **2005,** *127* (26), 9588-92.

44. Chen, J.; Leung, F. K.; Stuart, M. C. A.; Kajitani, T.; Fukushima, T.; van der Giessen, E.; Feringa, B. L., Artificial muscle-like function from hierarchical supramolecular assembly of photoresponsive molecular motors. *Nat Chem* **2018,** *10* (2), 132-138.

45. Luo, Y.; Shoichet, M. S., A photolabile hydrogel for guided three-dimensional cell growth and migration. *Nat Mater* **2004,** *3* (4), 249-53.

46. Lee, T. T.; Garcia, J. R.; Paez, J. I.; Singh, A.; Phelps, E. A.; Weis, S.; Shafiq, Z.; Shekaran, A.; Del Campo, A.; Garcia, A. J., Light-triggered in vivo activation of adhesive peptides regulates cell adhesion, inflammation and vascularization of biomaterials. *Nat Mater* **2015,** *14* (3), 352-60.

47. Li, L.; Scheiger, J. M.; Levkin, P. A., Design and Applications of Photoresponsive Hydrogels. *Adv Mater* **2019,** *31* (26), e1807333.

48. Maity, C.; Hendriksen, W. E.; van Esch, J. H.; Eelkema, R., Spatial structuring of a supramolecular hydrogel by using a visible-light triggered catalyst. *Angew Chem Int Ed Engl* **2015,** *54* (3), 998-1001.

49. Zhou, H.; Xue, C.; Weis, P.; Suzuki, Y.; Huang, S.; Koynov, K.; Auernhammer, G. K.; Berger, R.; Butt, H. J.; Wu, S., Photoswitching of glass transition temperatures of azobenzene-containing polymers induces reversible solid-to-liquid transitions. *Nat Chem* **2017,** *9* (2), 145-151.

Chapter 3

Supramolecular Interaction Form Tough and Self-Healing Hydrogels

3.1 Introduction

Hydrogel is crosslinked hydrophilic polymer networks with a large amount of water, which are widely existing in plant and animal tissues. Due to its unique solid and liquid properties, synthetic polymeric hydrogels are extensively developed and used in industrial, biomedical and environmental areas.[1-4] However, compared with natural hydrogels, which are tough to support the surrounding components, most of the synthetic polymeric hydrogels are either mechanical weak[5].

To date, many efforts have been done to improve the toughness of hydrogels by introducing dissipation energy into hydrogels.[6-8] For example, the strategy for double-network hydrogels to improve dissipation energy was utilization of fracture of polymer chains.[9, 10] Pullout of fibers or other fillers were used as mechanisms for energy dissipation in meso-/macro-scale composites hydrogels.[11] Moreover, hydrogels based on reversible crosslinkers can also dissipate a great amount of energy and exhibit fatigue-resistance in the meanwhile, which comes from the deconstruction and reconstruction of reversible crosslinkers.[5, 12, 13] In recent work, partial or completely

self-recoverable tough hydrogels have been reported by using ionic interaction,[14, 15] hydrogen bonds[16, 17] or hydrophobic interaction[18, 19] as recoverable sacrificed bonds.

In this work, we presented a model physical hydrogel system P(UM-*co*-NBOC) from the random copolymerization of two monomers, 2-ureidoethyl methacrylate (UM) and 2-nitrobenzyloxycarbonylaminoethyl methacrylate (NBOC) to realize this concept (Figure 3.1). As the side groups of UMA and NBOC are able to form multiple noncovalent bonds via hydrogen bonding and hydrophobic interaction, the physical hydrogel P(UM-*co*-NBOC) without covalent bonds density exhibits the high strength, toughness, and viscoelastic behavior.

3.2 Experimental

3.2.1 Materials

2-Nitrobenzyloxycarbonylaminoethyl methacrylate (NBOC) was synthesized according to literature.[20] 2-Ureidoethyl methacrylate (UM) was provided by Osaka chemicals Co., Ltd. 2,2′-Azobisisobutyronitrile (AIBN, 98%) was purchased from Sigma-Aldrich. N,N'-methylenebis (acrylamide) (MBAA) was purchased from Tokyo Kasei Co., Ltd. Dimethyl sulfoxide (DMSO) was purchased from Wako Pure Chemical Industries, Ltd. All chemicals were used as received.

3.2.2 Synthesis of hydrogels

The monomers with different monomer molar ratios were first dissolved in their co-solvent DMSO. For P(UM-*co*-NBOC) system, the pre-gel solution contains 1.5 M UM and NBOC, and 0.003 M AIBN (initiator).

The pre-gel solution was then poured into in a reaction cell consisting of a pair of glass plates with a spacer, and heated at 70 ℃ for 8 hours. After polymerization, the as-prepared gel was immersed in a large amount of water for 1 week to reach equilibrium. The hydrogels were named as polymer-f_{NBOC}, where f_{NBOC} was the molar fraction of NBOC.

3.2.3 Characterization of hydrogels

Swelling measurements

The as-prepared gel was cut into samples with fixed sizes and then immersed in a large amount of pure water until reaching equilibrium. The swelling volume ratio Q_v was defined as the ratio of the sample volume at swelling equilibrium V to that in the as-prepared state V_0, $Q_v = V/V_0$.

Water content

The water content (W_{water}, wt%) of hydrogel samples was measured with a moisture balance (MOC-120H, SHIMADZU Co., Japan) based on the equation, W_{water}=

*(m_{water}/m_{sample}) *100%*, where m_{water} *(g)* is the weight of water in the hydrogel network, and m_{sample} *(g)* is the weight of the whole hydrogel sample.

Mechanical test

Uniaxial tensile tests were performed on hydrogels using a tensile-compressive tester (Instron 5965 type universal testing system) in air. The cyclic tensile stress-strain measurements were performed using a tensile-compressive tester (Tensilon RTC-1310A, Orientec Co.) in a water bath to prevent water from evaporating from the samples. The dissipated energy, calculated by the hysteresis area (U_{hys}), and the hysteresis coefficient, the ratio of hysteresis area to the overall area below the loading curve, was named as U_{hys} coefficient.

All tests were carried out on dumbbell-shaped samples with the standard JIS-K6251-7 size (12 mm (L) × 2 mm (d) × 0.3–3 mm (w)). All samples were stretched along the length direction of the samples at a deformation rate of 100 mm/min.

3.3 Results and discussion

We first dissolve hydrophobic NBOC and hydrophilic UM into their co-solvent DMSO, and performed random radical polymerization at high monomer concentration so that the polymers formed are well above their entanglement concentration to obtain organogel. The polymer network is physically crosslinked by hydrogen bond provided

by UM residues. The organogel substantially immersed in water to remove the DMSO and unreacted monomers.

3.3.1 Effect of the fraction of NBOC (f_{NBOC})

During the solution replacement process, the NBOC residues aggregate into the hydrophobic domain working as physical crosslinks. Compared with the original organogel, the hydrogel at equilibrium state shrink due to the strong hydrogen bonds and the hydrophobic interaction between polymer chains (**Figure 3.1**). This phenomenon becomes more obvious with elevating the NBOC fraction (f_{NBOC}).

The formation of physical crosslinkers by hydrophobic interaction between NBOC residues significantly enhances the mechanical properties of hydrogel (**Figure 3.2**). With the increase of f_{NBOC}, the fracture stress of hydrogels increased, owing to the increasing amount of physical crosslinkers, while the fracture strain decreased when f_{NBOC} over 0.1 (**Figure 3.2**). The toughness of hydrogel, reflected by work of extension, enhanced gradually with increase in f_{NBOC}. For P(UM-*co*-NBOC)-0.2 hydrogels, the slight decrease in toughness was due to the sharp decrease in elongation. The increase of the amount of physical crosslinkers and decrease in volume of hydrogels leads to the higher density of physical crosslinkers with the increase in f_{NBOC}, which accounts for the dramatic increase in Young's modulus.

3.3.2 Effect of total monomer concentration (C_m)

To study the effect of total monomer concentration on the physical and mechanical properties of hydrogel, P(UM-*co*-NBOC) hydrogels with varied total monomer concentration were synthesized. Since the P(UM-*co*-NBOC)-0.15 hydrogel sample performing great mechanical properties (**Figure 3.2**), the fraction of NBOC was fixed at 0.15. As shown in **Figure 3.3**, with the monomer concentration increasing, the swelling ratio increase while there is no change in water content. Besides, the result of swelling ratio (Q_V) divided by total monomer concentration (C_m) kept constant, which implies the space of every polymer chain in the hydrogel sample occupied is same. The Young's modulus increase dramatically, but there is no obvious difference between fracture stress and strain, and work of extension. The change of total monomer concentration (C_m) showed no obvious influence on both of physical and mechanical properties of hydrogels, therefore, the total monomer concentration (C_m) was fixed at 1.5 mol/L.

3.3.3 Hysteresis and energy dissipation

To further investigating the hydrogels reinforced by hydrophobic interaction, loading-unloading tests were conducted to evaluate the hysteresis and energy dissipation of hydrogels (**Figure 3.4**). Distinct yielding and hysteresis were observed in the loading-

unloading cycle of hydrogels. U_{hys} and U_{hys} coefficient increased with the f_{NBOC} in P(UM-*co*-NBOC) hydrogels. It indicates that the energy used for deformation could be dissipated by breaking a large amount of hydrophobic interactions. For instance, the U_{hys} of P(UM-*co*-NBOC)-0.2 was 2.36 MJ/m^3 with a corresponding coefficient 72%, which is 25 times than that of pure PUM hydrogels (**Figure 3.4**).

The detached physical crosslinkers, by which energy can be dissipated during deformation of hydrogel samples, will reconstruct subsequently. Thus, the dynamic and reversible feature of physical crosslinkers endowed the hydrogel with good self-recovery behavior and fatigue resistance.

3.3.4 Self-recovery

Cyclic loading-unloading tensile tests were performed to investigate the self-recovery ability of P(UM-*co*-NBOC) hydrogels (**Figure 3.5**). P(UM-*co*-NBOC)-0.15 hydrogels was chosen as representative, because of their outstanding U_{hys} and U_{hys} coefficient of the first loading-unloading cycle. In 10 minutes, the hydrogel could recover to more than 80% of the virgin state; after 240 minutes, the hydrogel could recover to 100% of the virgin state (**Figure 3.5**). It is contributed by the physical cross-linkers of hydrophobic interaction and hydrogen bonds. The hydrogel sample showed obvious residual strain after unloading (**Figure 3.5**), which means the plastic deformation, while it would disappear after the relatively small waiting time (20 minutes). It inferred the

plastic deformation could be completely removed. The dependence of residual strain and hysteresis ratio on waiting time indicates the self-recovery included two stages, which is similar to polyampholyte hydrogels (PA hydrogels)[14] and polyion-complex hydrogels (PIC hydrogels).[15] This two-stage recovery process is related to the competition between the elasticity of the primary chain and the strength of temporarily reformed bonds during the unloading process.

3.4 Conclusion

By addition of hydrophobic interaction between NBOC moieties into hydrophilic PUM networks, supramolecular hydrogels based on hydrophobic interaction and hydrogen bonds, acting as crossliners. This special combination of physical bonds results in high toughness, stiffness, fatigue resistance, and high mechanical performance. The reversible crosslikers, renders the self-recovery of the materials. The effect of fraction of NBOC and total monomer concentration on physical and mechanical properties of hydrogels were investigated and optimized. Since the NBOC monomer has multiple stimuli-response, integrating the stimuli-response into the tough hydrogel could be conducted in further studies. Therefore, these gels might open new avenue of tough hydrogels.

Reference

1. Lee, K. Y.; Mooney, D. J., Hydrogels for Tissue Engineering. *Chemical Reviews* **2001,** *101* (7), 1869-1880.

2. Calvert, P., Hydrogels for Soft Machines. *Advanced Materials* **2009,** *21* (7), 743-756.

3. Kumacheva, E., Hydrogels: The catalytic curtsey. *Nat Mater* **2012,** *11* (8), 665-6.

4. Seliktar, D., Designing cell-compatible hydrogels for biomedical applications. *Science* **2012,** *336* (6085), 1124-8.

5. Zhao, X., Multi-scale multi-mechanism design of tough hydrogels: building dissipation into stretchy networks. *Soft Matter* **2014,** *10* (5), 672-687.

6. Sun, J. Y.; Zhao, X.; Illeperuma, W. R.; Chaudhuri, O.; Oh, K. H.; Mooney, D. J.; Vlassak, J. J.; Suo, Z., Highly stretchable and tough hydrogels. *Nature* **2012,** *489* (7414), 133-6.

7. Zhao, X., Designing toughness and strength for soft materials. *Proc Natl Acad Sci U S A* **2017**.

8. Ritchie, R. O., The conflicts between strength and toughness. *Nat Mater* **2011,** *10* (11), 817-22.

9. Gong, J. P.; Katsuyama, Y.; Kurokawa, T.; Osada, Y., Double-Network Hydrogels with Extremely High Mechanical Strength. *Advanced Materials* **2003,**

15 (14), 1155-1158.

10. Gong, J. P., Why are double network hydrogels so tough? *Soft Matter* **2010,** *6* (12).

11. Huang, Y.; King, D. R.; Sun, T. L.; Nonoyama, T.; Kurokawa, T.; Nakajima, T.; Gong, J. P., Energy-Dissipative Matrices Enable Synergistic Toughening in Fiber Reinforced Soft Composites. *Advanced Functional Materials* **2017,** *27* (9).

12. Lin, S.; Liu, X.; Liu, J.; Yuk, H.; Loh, H.-C.; Parada, G. A.; Settens, C.; Song, J.; Masic, A.; McKinley, G. H.; Zhao, X., Anti-fatigue-fracture hydrogels. *Science Advances* **2019,** *5* (1).

13. Gonzalez, M. A.; Simon, J. R.; Ghoorchian, A.; Scholl, Z.; Lin, S.; Rubinstein, M.; Marszalek, P.; Chilkoti, A.; López, G. P.; Zhao, X., Strong, Tough, Stretchable, and Self-Adhesive Hydrogels from Intrinsically Unstructured Proteins. *Advanced Materials* **2017,** *29* (10).

14. Sun, T. L.; Kurokawa, T.; Kuroda, S.; Ihsan, A. B.; Akasaki, T.; Sato, K.; Haque, M. A.; Nakajima, T.; Gong, J. P., Physical hydrogels composed of polyampholytes demonstrate high toughness and viscoelasticity. *Nat Mater* **2013,** *12* (10), 932-7.

15. Luo, F.; Sun, T. L.; Nakajima, T.; Kurokawa, T.; Zhao, Y.; Sato, K.; Ihsan, A. B.; Li, X.; Guo, H.; Gong, J. P., Oppositely charged polyelectrolytes form tough, self-healing, and rebuildable hydrogels. *Adv Mater* **2015,** *27* (17),

2722-7.

16. Phadke, A.; Zhang, C.; Arman, B.; Hsu, C. C.; Mashelkar, R. A.; Lele, A. K.; Tauber, M. J.; Arya, G.; Varghese, S., Rapid self-healing hydrogels. *Proc Natl Acad Sci U S A* **2012,** *109* (12), 4383-8.

17. Fan, H.; Wang, J.; Jin, Z., Tough, Swelling-Resistant, Self-Healing, and Adhesive Dual-Cross-Linked Hydrogels Based on Polymer–Tannic Acid Multiple Hydrogen Bonds. *Macromolecules* **2018,** *51* (5), 1696-1705.

18. Zhang, H. J.; Sun, T. L.; Zhang, A. K.; Ikura, Y.; Nakajima, T.; Nonoyama, T.; Kurokawa, T.; Ito, O.; Ishitobi, H.; Gong, J. P., Tough Physical Double-Network Hydrogels Based on Amphiphilic Triblock Copolymers. *Adv Mater* **2016,** *28* (24), 4884-90.

19. Chen, Q.; Zhu, L.; Chen, H.; Yan, H.; Huang, L.; Yang, J.; Zheng, J., A Novel Design Strategy for Fully Physically Linked Double Network Hydrogels with Tough, Fatigue Resistant, and Self-Healing Properties. *Advanced Functional Materials* **2015,** *25* (10), 1598-1607.

20. Wang, X.; Liu, G.; Hu, J.; Zhang, G.; Liu, S., Concurrent block copolymer polymersome stabilization and bilayer permeabilization by stimuli-regulated "traceless" crosslinking. *Angew Chem Int Ed Engl* **2014,** *53* (12), 3138-42.

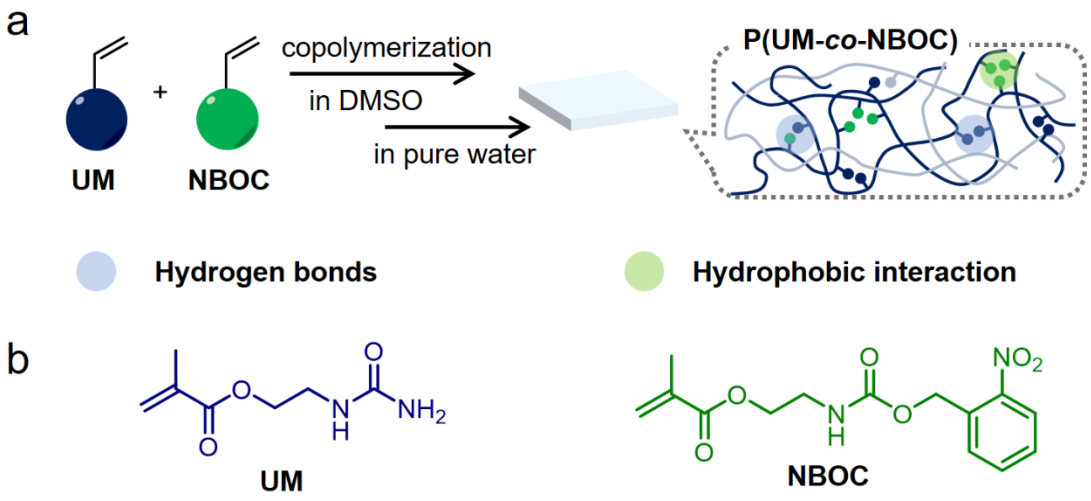


Figure 3.1 (a) Synthesis routine of P(UM-*co*-NBOC) hydrogel; (b) Chemical structure of monomers.

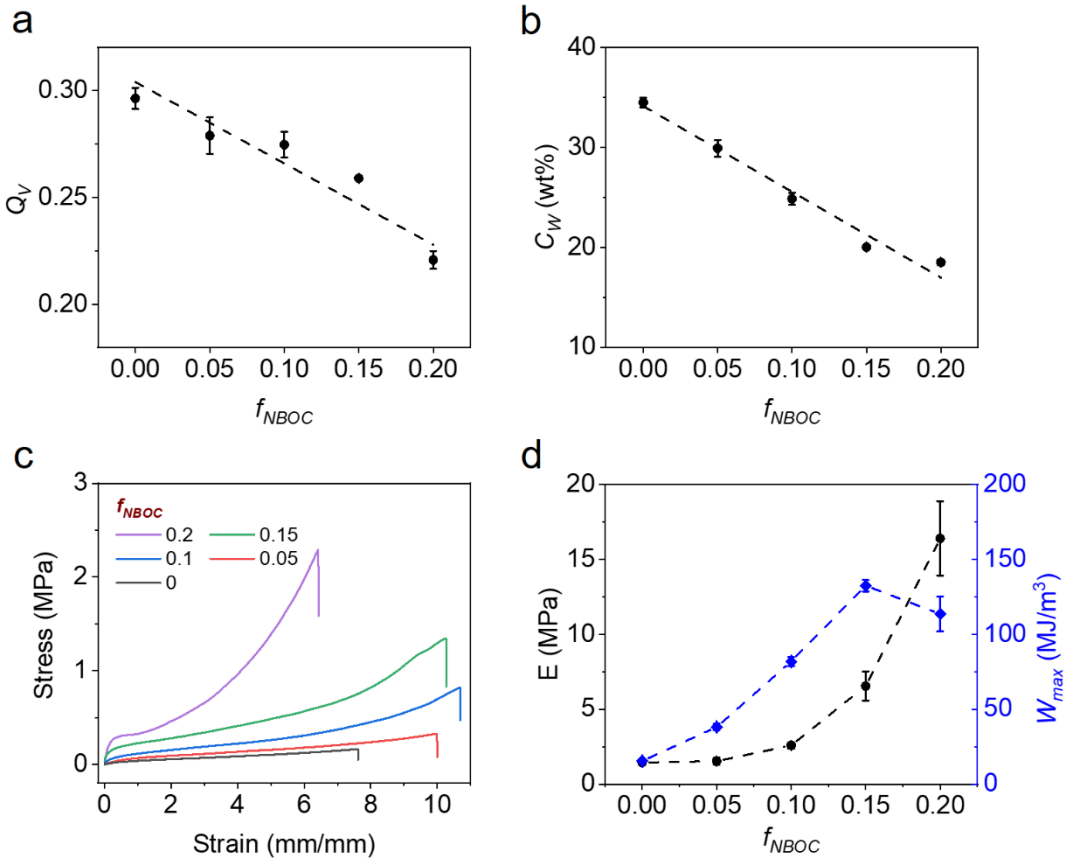


Figure 3.2 Physical properties and tensile behaviors for P(UM-*co*-NBOC) hydrogels. (a) Volume ratio of samples in water in relative to that in DMSO, Q_V, (b) water content, (c) tensile stress-strain curves, and (d) Young's modulus (E) and work of extension to fracture (W_{max}) of samples with different NBOC molar fraction f_{NBOC}. Each data was the average of 3-5 specimens of the same composition samples. Error bars represent standard deviation.

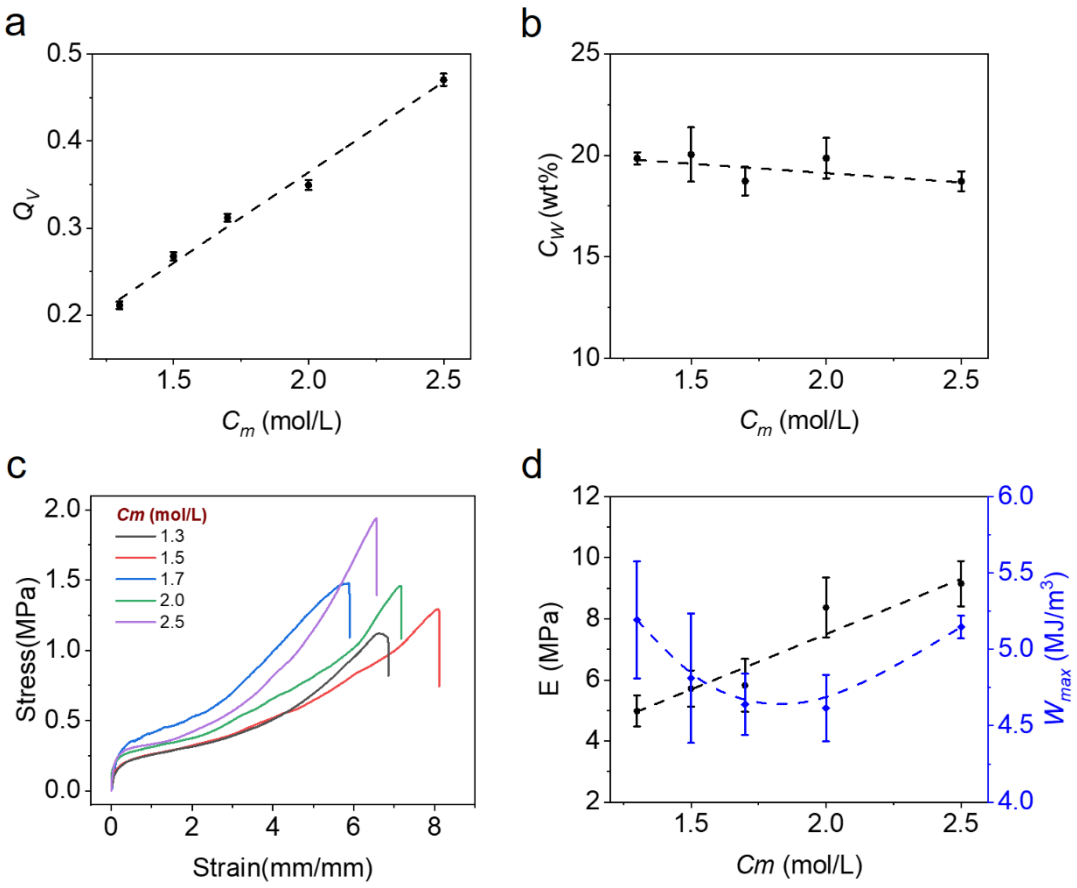


Figure 3.3 Physical properties and tensile behaviors for P(UM-*co*-NBOC) hydrogels. (a) Volume ratio of samples in water in relative to that in DMSO, Q_V, (b) water content, (c) tensile stress-strain curves, and (d) Young's modulus (E) and work of extension to fracture (W_{max}) of samples with different total monomer concentration C_m (mol/L). Each data was the average of 3-5 specimens of the same composition samples. Error bars represent standard deviation.

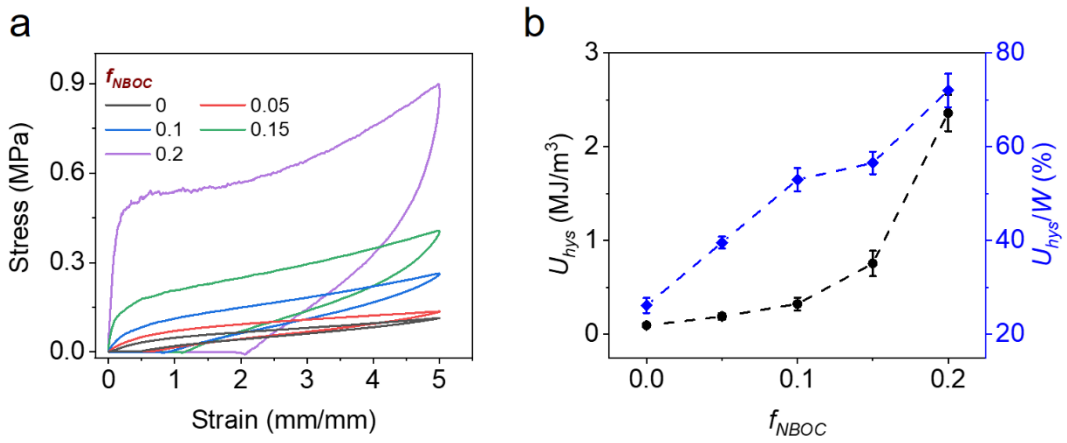


Figure 3.4 Hysteresis behavior of P(UM-*co*-NBOC) hydrogels. (a) loading-unloading curves, (b) dissipated energy (U_{hys}) calculated from the hysteresis area and energy dissipation coefficient (U_{hys}/W) of hydrogels with different f_{NBOC} for a strain of 5. Each data was the average of 3-5 specimens of the same composition samples. Error bars represent standard deviation.

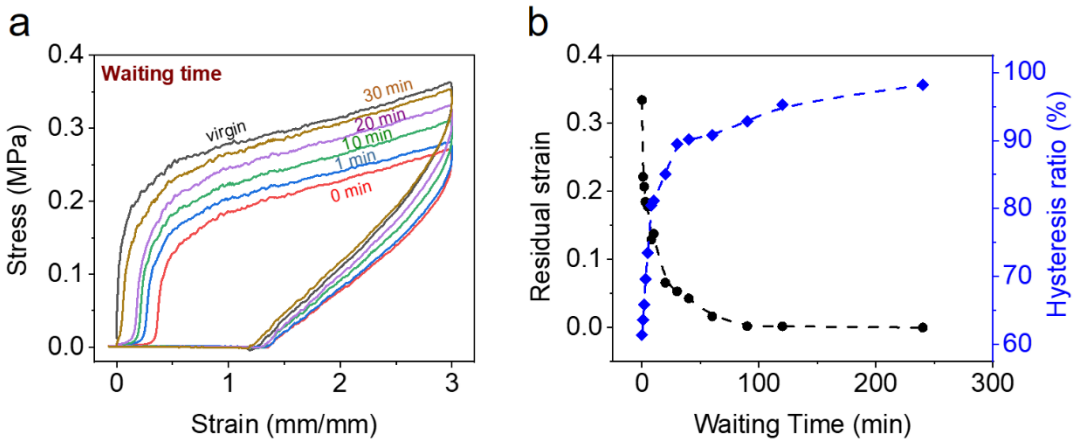


Figure 3.5 Self-recovery of P(UM-*co*-NBOC) hydrogels.(a) Cyclic loading-unloading curves and (b) residual strain and hysteresis recovery ratio between the second and first loading cycles for different waiting times of sample with f_{NBOC} = 0.15.

Chapter 4

Fabrication of tough hydrogels composites from photo-responsive polymers to show double network effect

4.1 Introduction

Since the first report of double-network (DN) hydrogel in 2003[1], which has high strength and toughness but containing 90% water, the tough soft matters (hydrogels and elastomers) have achieved great development based on DN concept[2-6]. For instance, the failure stress for DN-type hydrogels can easily reach to tens of MPa nowadays[7]. Meanwhile, the toughening mechanism of DN hydrogels have been investigated for many years[8, 9]. It is clarified that the special interpenetrated network structure in DN gels plays the key role in toughening mechanism. Specifically, a DN gel has two polymer networks of very different structure and properties: a densely crosslinked, fully stretched network from polyelectrolyte (the first network, as rigid skeleton) and a sparsely crosslinked, modestly stretched network from neutral polymer (the second network, as ductile substance). During deformation, the first network (rigid skeleton) ruptures into fragmentation first, while the second network (ductile substance) maintains the integrity and gives large extension of the materials after the fracture of the first network. Thus, the covalent bonds of the first network act as sacrificial bonds

and the second network chains act as hidden length. Such fracture process, referred to as internal fracture, macroscopically appears as mechanical yielding[10], which is accompanied with a necking phenomenon. The latter is regarded as the coexistence of the damaged and undamaged zones[3, 11]. Based on the phenomenon, various models and hypothesis has been proposed to explain the molecular mechanism of DN gels[3, 4, 7, 8]. However, the direct observation of the internal fracture morphology of DN gels, at micrometer scale, is still unachievable.

Inspired by the strategy of DN gels, tough composites from two mechanically different components were developed, applying similar toughening mechanism of DN gels in macro-scale [12-14]. For example, Feng *et al*. fabricated a soft composite consisting of a macro-scale nylon fabric mesh as the rigid component and VHB^{TM} tape layers as soft component, and found that the deformation process is similar to that of DN gel: the fabric mesh fragmented into small islands surrounded by the highly stretched tapes[12]. Recently, our group also developed composites by combining low-melting-point alloy with macro-scale honeycomb structure and hydrogels[13], and observed the multi-step damage process of the rigid honeycomb alloy, similar to that of the DN gels. These results indicate that the macro-scale composites possess the same mechanical feature and toughening mechanism to the DN gels that are nano-scale composites.

In this work, we intend to develop macro-scale hydrogel composites showing the double network effect. There are several challenges. First, the soft matrix must be highly stretchable and possess a higher strength than the rigid skeleton[12-14]. Otherwise, the

fracture of the rigid skeleton causes catastrophic failure of the material without showing multi-step fracture of the rigid skeleton. Therefore, we need to develop energy-dissipated tough hydrogels as soft matrix, by introduction of reversible crosslinkers[13, 15]. The swelling mismatching and interface between the soft and rigid phases present another challenge for the hydrogel composites. The interface between heterogeneous phases in composite materials plays an essential role in force transmission and dissipation of energy, resulting in effective reinforcement on the mechanical properties[16]. In general, hydrogel composites are formed by polymerization in the presence of hard phases such as particles, fibers and layer elements as the reinforcing components[15, 17, 18], where the rigid surface and hydrogels are usually integrated by chemical anchoring or physical adhesion[19-25]. The swelling mismatch between soft and rigid phases lead to surface wrinkle, bulk deformation or even fracture of materials[26-28]. To overcome the difficulties mentioned above, we present a facile strategy to prepare hydrogel composites with continuous interface by designing and develop photo-responsive polymers (**Figure 4.1**). We synthesized copolymers from hydrophilic 2-ureidoethyl methacrylate (UM) and hydrophobic photo-responsive (2-nitrobenzyloxycarbonylaminoethyl methacrylate, NBOC) (**Figure 4.1**). The NBOC residues in the P(UM-co-NBOC) copolymers play two roles. One is working as physical crosslinkers based on their hydrophobic association, which can dissipate a large amount of energy during deformation so that toughen the hydrogels; the other is providing photo-responsiveness to switch the physical crosslinking to chemical crosslinking[29].

Upon UV irradiation, the 2-nitrobenzyl functional group of NBOC exhibits photo-labile characteristics, with the release of 2-nitrobenzaldehyde and CO_2. In this process, the hydrophobic NBOC groups transform into hydrophilic 2-aminoethyl methacrylate (AMA), leading to disassembly of physical crosslinkers by hydrophobic interaction. However, the resultant amino groups of AMA would further attack close-by ester bonds of UM to form new chemical crosslinkers. As a result, after UV irradiation, the physical P(UM-*co*-NBOC) gels transform to chemical P(UM-*co*-AMA) gels without significant change in swelling ratio. Such photo-switching of physical gels to chemical gels brings about a dramatic change in the mechanical behavior of the hydrogels from soft and highly stretchable to rigid and less stretchable. By controlling the UV irradiation, the NBOC-based hydrogels can be easily reconstructed into various composites. As an example, we fabricated sandwich hydrogels composed of rigid chemical hydrogel in the outer layers and soft physical hydrogel in the middle layer. The composite hydrogels, having a strong interface and negligible swelling mismatching, are mechanically tough showing feature similar with the DN hydrogels[1, 3-6], where the hard layers, P(UM-*co*-AMA), play a role of the first network, imparting high modulus and rupturing to dissipate energy, and the soft layer, P(UM-*co*-NBOC), plays a role of the second network, maintaining the global integrity. The macro-scale fracture process of this composite gives insight to understand the micro-scale fracture process of DN gels.

4.2 Experimental

4.2.1 Materials

2-Nitrobenzyloxycarbonylaminoethyl methacrylate (NBOC) was synthesized according to literature.[29] 2-Ureidoethyl methacrylate (UM) was provided by Osaka chemicals Co., Ltd. 2,2′-Azobisisobutyronitrile (AIBN, 98%) was purchased from Sigma-Aldrich. Dimethyl sulfoxide (DMSO) was purchased from Wako Pure Chemical Industries, Ltd. All chemicals were used as received.

4.2.2 Synthesis of hydrogels

The monomers with different monomer molar ratios were first dissolved in their co-solvent DMSO. For P(UM-*co*-NBOC) system, the pre-gel solution contains 1.5 M monomers of UM and NBOC mixture with proscribed NBOC molar fraction (f_{NBOC}), and 0.003 M AIBN (initiator). The total monomer concentration was chosen high enough so that the polymers formed are well above their entanglement concentration. The pre-gel solution was then poured into in a reaction cell consisting of a pair of glass plates with a spacer of prescribed thickness, and the reaction cell was heated at 70 ℃ for 8 hours for thermal initiated polymerization. After polymerization, the as-prepared gel was immersed in a large amount of water for 1 week to reach equilibrium. The

hydrogels were coded as P(UM-*co*-NBOC)-f_{NBOC}.

4.2.3 Characterization of hydrogels

Swelling ratio measurements

The as-prepared gel was cut into samples with prescribed sizes and then immersed in a large amount of pure water until reaching equilibrium. The swelling volume ratio Q_v was defined as the ratio of the sample volume at swelling equilibrium V to that in the as-prepared state V_0, $Q_v = V/V_0$.

Water content measurement

The water content (C_w, wt%) of hydrogel samples were measured with a moisture balance (MOC-120H, SHIMADZU Co., Japan) based on the equation, $C_w = (m_w/m_g) * 100\%$, where m_w *(g)* is the weight of water in the hydrogel network, and m_g *(g)* is the weight of the whole hydrogel sample.

Mechanical test

Uniaxial tensile tests were performed on hydrogels using a tensile-compressive tester (Instron 5965 type universal testing system) in air. The cyclic tensile stress-strain measurements were performed using a tensile-compressive tester (Tensilon RTC-1310A, Orientec Co.) in a water bath to prevent water from evaporating from the

samples. The dissipated energy (U_{hys}) at a prescribed deformation was calculated from the hysteresis area, and the fraction of dissipated energy in relative to total energy applied to the sample (U_{hys}/W) was calculated from the ratio of hysteresis area U_{hys} to the overall area W below the loading curve. W is the work of extension for a prescribed deformation. The hysteresis ratio was calculated from the ratio of hysteresis area in the prescribed cycle U_{hys} to the hysteresis area U_{hys} of the first cycle in the cyclic loading-unloading test.

All tests were carried out on dumbbell-shaped samples with the standard JIS-K6251-7 size (12 mm (L) × 2 mm (d)). The sample thickness was 0.3–3 mm (w) depending on the thickness of the reaction cell spacer and the sample formulation. All tests were performed at a deformation velocity of 100 mm/min, corresponding to a stretch rate of 0.14 s^{-1}.

UV irradiation for chemical crosslinking

UV irradiation on samples was conducted on a UV-LED irradiation panel (UAW365-31110-1212F, Sentech Co.). The intensity of UV irradiation was 1.78×10^4 mJ/cm^2. The hydrogel samples were immersed in a cell of water to prevent water evaporation from the samples during irradiation. The cell consists of a pair of glass plates with a spacer. Fourier transform infrared (FT-IR) spectra were recorded on a Bruker VECTOR-22 IR spectrometer.

Optical microscope observation

To observe the microcrack formation under stretching, the hydrogel samples after UV irradiation were fixed under various elongation ratios by a tailor-made stretching device[30], and were observed under an optical microscope (Nikon, Eclipse, LV100POL).

Puncture test

A needle was fixed on the load cell, and the hydrogels were fixed in the molds under water (**Figure 4.2**), which composed of silica spacer (less than the thickness of samples) and two glass plates with small poles (diameter: 0.5 mm). All tests were carried on square samples (10 mm × 10 mm × ~1 mm). The insertion velocity during penetration was maintained at 100 mm/min.

4.3 Results and discussion

4.3.1 Contrast of physical properties of hydrogel before and after UV irradiation

Upon UV irradiation, the 2-nitrobenzyl function group of NBOC exhibits photo-labile characteristics, with the release of 2-nitrobenzaldehyde and CO_2. In this process, the hydrophobic NBOC transforms into hydrophilic moieties, leading to disassembly of physical crosslinkers composed of hydrophobic interaction, However, the resultant amino groups (2-AMA) would further attack close-by ester bonds to generate new

chemical crosslinkers (**Figure 4.1**).

The hydrogel with newly formed network (name as P(UM-*co*-AMA)) is yellow due to the color of by-product of 2-nitrobenzaldehyde (**Figure 4.3**). After hydrogel reaching equilibrium in DI water, there was no significant change in volume of hydrogels before and after UV irradiation (**Figure 4.3 and 4.4**), indicating that the physical crosslinkers are supposed to be just replaced by the newly formed chemical crosslinkers.

4.3.2 Contrast of mechanical properties of hydrogel before and after UV irradiation

Tensile tests were conducted to measure the mechanical properties of P(UM-*co*-AMA) hydrogel (**Figure 4.5**). Compared with the hydrogel before UV irradiation, P(UM-*co*-AMA) performed much shorter fracture strain but higher Young's modulus, about twice the modulus of samples before UV irradiation (**Figure 4.5**), which is attributed to the newly formed chemical crosslinkers. From the contrast of modulus of hydrogel samples before and after UV irradiation, we could easily utilize the UV irradiation to adjust the modulus of samples *in situ*.

4.3.3 The effect of factors of UV irradiation on hydrogel samples properties after UV irradiation

The UV triggered chemical crosslinking could be modulated by control of UV irradiation intensity and duration. Thus, the physical and mechanical properties of hydrogel samples with different UV irradiation intensity and duration were tested to study the different effect of factors of UV irradiation on properties of hydrogel samples after UV irradiation.

Firstly, P(UM-*co*-NBOC) hydrogels (f_{NBOC} 0.15) with varied UV intensity were prepared. As shown in **Figure 4.6**, the color of samples became darker with the increase of UV intensity, due to the by-product of self-immolative reaction. However, there was slight difference between these samples in their stress-strain curve, which indicates the slight increase in chemical crosslinkers. It is supposed that the UV triggered self-immolative reaction would be continued with the increase of UV intensity, while the effective crosslinking would be kept constant. Thus, the UV intensity was fixed at 1.78 $\times 10^4$ mJ/cm^2.

Next, P(UM-*co*-NBOC) hydrogels (f_{NBOC} 0.15) over varied UV duration were prepared. The color of samples became darker with the increase of UV duration (**Figure 4.7**). In addition, FTIR spectroscopy of P(UM-*co*-NBOC) hydrogels (f_{NBOC} 0.15) after UV irradiation further corroborated UV-triggered carbamate decaging and crosslinking reactions. The absorbance peaks characteristic of nitro (1345 cm^{-1} and 1528 cm^{-1}) moieties disappeared after irradiation, revealing the photo-cleavage of o-nitrobenzyl groups; the absorbance intensity of ester carbonyl moieties (~1730 cm^{-1}) considerably decreased, which is accompanied with the increase of characteristic amide carbonyl

absorbance peak at ~1640 cm^{-1}), clearly suggesting the formation of amide linkages via either intrachain or interchain pathways; note that the latter case will contribute to effective chemical crosslinking. The tensile test showed both of the fracture stress and strain decreased with the increase in UV duration[29].

4.3.4 The formation of composite hydrogel

However, the ability of UV light penetration is limited, so that the UV light could not penetrate the whole hydrogel if the hydrogel is too thick. The depth of UV irradiation depends on the illumination time, which increased with exposure time extended, but reach to saturated depth after 30 min irradiation (**Figure 4.8**). It should be noticed that expose the hydrogel under strong UV light longer than 10 min leading to very high temperature (> 60 ºC), which may generate massive adverse reactions. Therefore, for the following samples we only expose the hydrogel under UV light for 10 min. For P(UM-*co*-NBOC) hydrogels with different f_{NBOC}, the depth of UV irradiation (10 min) kept around 152 nm, implying there is no relationship between f_{NBOC} and P(UM-*co*-AMA) thickness (**Figure 4.8**).

Based on such feature, the thick P(UM-*co*-NBOC) hydrogels can be transformed into hieratical hydrogels with different modulus region. For instance, after UV irradiation on both sides, the hydrogel showed “sandwich-like” structure with P(UM-*co*-AMA) surface (~150 μm) and P(UM-*co*-NBOC) matrix (**Figure 4.8**). While irradiate on one

side, we got a Janus type of hydrogel. All these hydrogels show no obvious change in volume at equilibrium state.

We use puncture test to confirm the different modulus region of hieratical hydrogels (**Figure 4.9**). The peaks of the curve mean the rupture occurred during the insertion process, inferring the needle punctured into another tissue with different mechanical properties.[31] In our case, although there is no obvious boundary between the so-called surface and matrix, obvious peaks origin from different layers were detected in hieratical hydrogels with low f_{NBOC} (0.05). However, for the hydrogels with high f_{NBOC} (> 0.05), the insertion force curves are quite different, only shows one peak in each system (**Figure 4.10**), which may be caused by their higher modulus on both surfaces and matrix. The puncture process includes generation and propagation of cracks and shear fracture, when the hydrogel shows high modulus, the cracks will propagate quickly cross the P(UM-*co*-AMA)/P(UM-*co*-NBOC) interface, leading to observation of only one rupture peak (**Figure 4.11**).

4.3.5 The mechanical properties of composite hydrogel

Next, we investigated the mechanical properties of sandwich hydrogels. **Figure 4.12** shows the stress-strain curves of sandwich hydrogels with varied f_{NBOC}. With the increase of f_{NBOC}, the fracture stress, fracture strain, and Young's modulus increased dramatically, due to the enhancement of crosslinker densities.

The UV irradiated samples with a sandwich structure can be treated as layered composites. To investigate the mechanical properties of the composite hydrogels, a series of P(UM-*co*-NBOC)-0.15 hydrogels with different thickness were irradiated with UV for 10 min. As the UV curing thickness was kept constant (~150 μm), the thickness ratio of hard outer layers to the soft middle layer was tuned by changing the overall sample thickness (**Figure 4.13**). The tensile behaviors of samples with different thickness ratio are shown in **Figure 4.13**. The one-component gels, of soft layer only (0/100) or hard layer only (100/0), showed single yielding point, while a very remarkable second yielding point was observed for all the sandwich gels at a strain of 1.6-1.8. With the increase of the thickness ratio of hard outer layers to soft middle layer, the stress at the 2nd yielding point increased while the fracture strain decreased, which could be also obviously witnessed in **Figure 4.14** for the fracture force. The composite hydrogels follow the stress and strain curve of the pure hard sample (100/0) at small strains and then deviated to show lower stresses at large strains. It is interesting to see that the strain for the 2nd yielding point was lower than the fracture strain of the homogeneous rigid sample (100/0), and decreased with the increase of the soft middle layer thickness. This result suggests that the soft middle layer makes the rigid outer layers break at a smaller strain in comparison with the free-standing rigid layer. The final fracture strain of the composites decreased with the increase of the hard/soft thickness ratio. The thinner the soft middle layer, the weaker the ability to bear the stretching and maintain global integrity. This is similar with the effect of the second

network in DN gels. It has been shown that if the concentration of 2nd network is not high enough, then the gel would not be toughened effectively. These results could also explain the difference in tensile tests between sandwich-like composite hydrogels with varied UV duration (**Figure 4.7**).

To reveal the fracture process, we further use optical microscopy to observe the structure change during the tensile process of the sandwich hydrogel (**Figure 4.15**). The pristine soft hydrogel (0/100) before UV curing deformed homogeneously without crack formation before sample failure, while the rigid sample (100/0) showed craze above the first necking, and with the increase of strain the craze density increased. The sandwich sample (95/5) showed well-defined dense crazes perpendicular to the elongation direction even at the very beginning of elongation (strain 0.1), corresponding to the first yielding point. The craze developed into branches with the increase of strain. With the increase of thickness of soft layer, both of craze perpendicular to the elongation direction and random irregular craze coexisted on the surface of sandwich sample (45/55). The increased soft layer maintained the integrity of the whole sample, thus the sample would not quickly break after the perpendicular craze grew into branches. On the other hand, the sandwich sample (30/70) showed irregular craze even at small strains (0.1), and at strain 2, above the 2nd yielding point in the tensile curve, the hard outer layer broke into small fragments, and the soft middle layer became visible. With the further increase of strain, strong strain localization in the soft middle layer was observed. This result clearly shows that the hard layers, sustaining most of the load,

broke first while the soft middle layer maintained the integrity. The irregular craze in sample (30/70) means that the cracks generated in the hard and less stretchable outer layers did not propagate since the middle layer, with increased strength, effectively carries the load.

It should be mentioned that even for the rigid 100/0 sample of 0.29 mm-thick, it showed surface craze before breaking (**Figure 4.15**). This is due to the gradient chemical crosslinking within the rigid layer. As shown in **Figure 4.16**, when the sample thickness varies from 0.14 mm (=70 μm x 2) to 0.29 mm (= 145 μm x 2), the sample softened, in accompany with an increase in the fracture strain and decrease in fracture stress. Furthermore, more surface crack appeared before sample failure for the thick sample. These results indicate the effect of gradient structure on the behavior of the 100/0 sample of 0.29 mm-thick.

The yielding phenomenon has some common features with the yielding phenomenon in double-network (DN) gels. For DN gels, there is no strain localization before yielding point. After yielding point, part of the sample constricts as necking zone, which subsequently grows with an increase in strain, and finally develops to the whole sample.[8] For our sandwich hydrogels, the appearance of the first percolated crack is reflected as the first yielding point and the crazing or fragmentation of the hard layers in the stress-strain curve, and the elongation of the middle layer between the cracks of the outer layers is resemble to the elongation of the second network in the necking zones of DN gels. In DN gels, usually, only one necking zone is generated and then it grows,

while in the sandwich hydrogels, the crazes are generated over the whole sample surfaces. Such differences correspond to the yielding point and broad yielding peak in stress-strain curves for DN gels and for sandwich hydrogels, respectively. This study shows that when the soft layer is relatively thin and weak, strip cracks are formed in the hard layers after yielding and the crack branches to break the layer into irregular fragmentation at enhanced strain. When the soft layer is relatively thick and strong, the crack grows irregularly to form irregular fragmentation right after yielding. The direct observation of the fracture process of the hard layers suggests that the internal fracture morphology of the first network in DN hydrogels would depend on the second network concentration.

4.3.6 Hysteresis and energy dissipation of composite hydrogel

Loading-unloading tests were conducted to evaluate the energy dissipation and energy dissipation coefficient of sandwich hydrogels (30/70) (**Figure 4.17**). The sandwich hydrogel showed much larger hysteresis than its original P(UM-*co*-NBOC) gel in the first loading-unloading cycle (**Figure 3.4**). It indicated more dissipation of energy contributed by the newly formed chemical crosslinkers instead of physical crosslinkers. The hysteresis area enclosed by the first loading-unloading cycle is up to 64% of the work of extension, while that for hydrogel before UV irradiation is 56%, which is consistent with the results before. However, the sandwich hydrogel cannot fully recover

due to its chemical crosslinked network origin (**Figure 4.17**). The residual strain and hysteresis showed dependence with waiting time, and the recovery also included two stages, however, the hysteresis ratio reached only 38% of the hysteresis area in first loading-unloading cycle (**Figure 4.17**). This is related to the break of unrecoverable primary chains after UV irradiation.

4.3.7 Patterned composite hydrogel

Since UV light can be easily controlled, we further use UV mask to fabricate the pattern hydrogels with different modulus regions. For instance, a 2D-patterned hydrogel, composed of alternating P(UM-*co*-NBOC) and P(UM-*co*-AMA) structure, was prepared from thin P(UM-*co*-NBOC) hydrogel, which UV light could penetrate the whole sample (**Figure 4.18**). It showed similar Young's modulus and fracture strain compared with the pure P(UM-*co*-AMA) samples, while there was a yielding near the fracture strain, which is because of the structure macro-scale composite materials. When we irradiate a thick P(UM-*co*-NBOC) gel with UV mask, a 3D-patterned hydrogel can be fabricated, which structure can be regard as two slices of 2D-patterned gels with a P(UM-*co*-NBOC) gel between them. The tensile stress-strain curve of 3D-patterned hydrogel shows very similar with that of sandwich-like hydrogels (**Figure 4.18**).

4.4 Conclusion

Based on the addition of hydrophobic interaction by copolymerization with NBOC, mechanical properties, toughness and fatigue resistance of P(UM-*co*-NBOC) hydrogels improved dramatically. Upon UV irradiation, part of physical crosslinkers composed of hydrophobic interaction transformed into chemical crosslinkers, which further enhance the mechanical properties. By control the UV irradiation depth and position, hybrid hydrogel consisted of different modulus regions can be easily prepared. This work provides a new strategy to fabrication tough hydrogel composites by incorporating a photo-responsive hydrophobic residue into the hydrogel network.

Reference

1. Gong, J. P.; Katsuyama, Y.; Kurokawa, T.; Osada, Y., Double-Network Hydrogels with Extremely High Mechanical Strength. *Advanced Materials* **2003,** *15* (14), 1155-1158.

2. Tsukeshiba, H.; Huang, M.; Na, Y. H.; Kurokawa, T.; Kuwabara, R.; Tanaka, Y.; Furukawa, H.; Osada, Y.; Gong, J. P., Effect of polymer entanglement on the toughening of double network hydrogels. *J Phys Chem B* **2005,** *109* (34), 16304-9.

3. Na, Y.-H.; Tanaka, Y.; Kawauchi, Y.; Furukawa, H.; Sumiyoshi, T.; Gong,

J. P.; Osada, Y., Necking Phenomenon of Double-Network Gels. *Macromolecules* **2006,** *39* (14), 4641-4645.

4. Huang, M.; Furukawa, H.; Tanaka, Y.; Nakajima, T.; Osada, Y.; Gong, J. P., Importance of Entanglement between First and Second Components in High-Strength Double Network Gels. *Macromolecules* **2007,** *40* (18), 6658-6664.

5. Na, Y.-H.; Kurokawa, T.; Katsuyama, Y.; Tsukeshiba, H.; Gong, J. P.; Osada, Y.; Okabe, S.; Karino, T.; Shibayama, M., Structural Characteristics of Double Network Gels with Extremely High Mechanical Strength. *Macromolecules* **2004,** *37* (14), 5370-5374.

6. Nakajima, T.; Furukawa, H.; Tanaka, Y.; Kurokawa, T.; Osada, Y.; Gong, J. P., True Chemical Structure of Double Network Hydrogels. *Macromolecules* **2009,** *42* (6), 2184-2189.

7. Gong, J. P., Why are double network hydrogels so tough? *Soft Matter* **2010,** *6* (12).

8. Nakajima, T.; Kurokawa, T.; Ahmed, S.; Wu, W.-l.; Gong, J. P., Characterization of internal fracture process of double network hydrogels under uniaxial elongation. *Soft Matter* **2013,** *9* (6), 1955-1966.

9. Ahmed, S.; Nakajima, T.; Kurokawa, T.; Anamul Haque, M.; Gong, J. P., Brittle–ductile transition of double network hydrogels: Mechanical balance of two networks as the key factor. *Polymer* **2014,** *55* (3), 914-923.

10. Matsuda, T.; Nakajima, T.; Fukuda, Y.; Hong, W.; Sakai, T.; Kurokawa,

T.; Chung, U.-i.; Gong, J. P., Yielding Criteria of Double Network Hydrogels. *Macromolecules* **2016,** *49* (5), 1865-1872.

11. Wang, X.; Hong, W., Pseudo-elasticity of a double network gel. *Soft Matter* **2011,** *7* (18).

12. Feng, X.; Ma, Z.; MacArthur, J. V.; Giuffre, C. J.; Bastawros, A. F.; Hong, W., A highly stretchable double-network composite. *Soft Matter* **2016,** *12* (44), 8999-9006.

13. Takahashi, R.; Sun, T. L.; Saruwatari, Y.; Kurokawa, T.; King, D. R.; Gong, J. P., Creating Stiff, Tough, and Functional Hydrogel Composites with Low-Melting-Point Alloys. *Adv Mater* **2018,** *30* (16), e1706885.

14. Cooper, C. B.; Joshipura, I. D.; Parekh, D. P.; Norkett, J.; Mailen, R.; Miller, V. M.; Genzer, J.; Dickey, M. D., Toughening stretchable fibers via serial fracturing of a metallic core. *Sci Adv* **2019,** *5* (2), eaat4600.

15. Huang, Y.; King, D. R.; Sun, T. L.; Nonoyama, T.; Kurokawa, T.; Nakajima, T.; Gong, J. P., Energy-Dissipative Matrices Enable Synergistic Toughening in Fiber Reinforced Soft Composites. *Advanced Functional Materials* **2017,** *27* (9).

16. Gojny, F. H.; Wichmann, M. H. G.; Fiedler, B.; Bauhofer, W.; Schulte, K., Influence of nano-modification on the mechanical and electrical properties of conventional fibre-reinforced composites. *Composites Part A: Applied Science and Manufacturing* **2005,** *36* (11), 1525-1535.

17. Cheng, Q.; Li, M.; Jiang, L.; Tang, Z., Bioinspired layered composites based on flattened double-walled carbon nanotubes. *Adv Mater* **2012,** *24* (14), 1838-43.

18. Huang, T.; Xu, H. G.; Jiao, K. X.; Zhu, L. P.; Brown, H. R.; Wang, H. L., A Novel Hydrogel with High Mechanical Strength: A Macromolecular Microsphere Composite Hydrogel. *Advanced Materials* **2007,** *19* (12), 1622-1626.

19. Sudre, G.; Olanier, L.; Tran, Y.; Hourdet, D.; Creton, C., Reversible adhesion between a hydrogel and a polymer brush. *Soft Matter* **2012,** *8* (31).

20. Keplinger, C.; Sun, J. Y.; Foo, C. C.; Rothemund, P.; Whitesides, G. M.; Suo, Z., Stretchable, transparent, ionic conductors. *Science* **2013,** *341* (6149), 984-7.

21. Sun, J. Y.; Keplinger, C.; Whitesides, G. M.; Suo, Z., Ionic skin. *Adv Mater* **2014,** *26* (45), 7608-14.

22. Yang, C. H.; Chen, B. H.; Lu, J. J.; Yang, J. H.; Zhou, J. X.; Chen, Y. M.; Suo, Z. G., Ionic cable. *Extreme Mechanics Letters* **2015,** *3*, 59-65.

23. Han, L.; Lu, X.; Liu, K.; Wang, K.; Fang, L.; Weng, L. T.; Zhang, H.; Tang, Y.; Ren, F.; Zhao, C.; Sun, G.; Liang, R.; Li, Z., Mussel-Inspired Adhesive and Tough Hydrogel Based on Nanoclay Confined Dopamine Polymerization. *ACS Nano* **2017,** *11* (3), 2561-2574.

24. Yuk, H.; Zhang, T.; Parada, G. A.; Liu, X.; Zhao, X., Skin-inspired hydrogel-elastomer hybrids with robust interfaces and functional microstructures. *Nat Commun* **2016,** *7*, 12028.

25. Yuk, H.; Zhang, T.; Lin, S.; Parada, G. A.; Zhao, X., Tough bonding of hydrogels to diverse non-porous surfaces. *Nat Mater* **2016,** *15* (2), 190-6.

26. Zhang, X.; Pint, C. L.; Lee, M. H.; Schubert, B. E.; Jamshidi, A.; Takei, K.; Ko, H.; Gillies, A.; Bardhan, R.; Urban, J. J.; Wu, M.; Fearing, R.; Javey, A., Optically- and thermally-responsive programmable materials based on carbon nanotube-hydrogel polymer composites. *Nano Lett* **2011,** *11* (8), 3239-44.

27. Kim, M.; Jung, B.; Park, J. H., Hydrogel swelling as a trigger to release biodegradable polymer microneedles in skin. *Biomaterials* **2012,** *33* (2), 668-78.

28. Tanaka, T.; Sun, S. T.; Hirokawa, Y.; Katayama, S.; Kucera, J.; Hirose, Y.; Amiya, T., Mechanical Instability of Gels at the Phase-Transition. *Nature* **1987,** *325* (6107), 796-798.

29. Wang, X.; Liu, G.; Hu, J.; Zhang, G.; Liu, S., Concurrent block copolymer polymersome stabilization and bilayer permeabilization by stimuli-regulated "traceless" crosslinking. *Angew Chem Int Ed Engl* **2014,** *53* (12), 3138-42.

30. Fukao, K.; Nonoyama, T.; Kiyama, R.; Furusawa, K.; Kurokawa, T.; Nakajima, T.; Gong, J. P., Anisotropic Growth of Hydroxyapatite in Stretched Double Network Hydrogel. *ACS Nano* **2017,** *11* (12), 12103-12110.

31. Jiang, S.; Li, P.; Yu, Y.; Liu, J.; Yang, Z., Experimental study of needle-tissue interaction forces: effect of needle geometries, insertion methods and tissue characteristics. *J Biomech* **2014,** *47* (13), 3344-53.

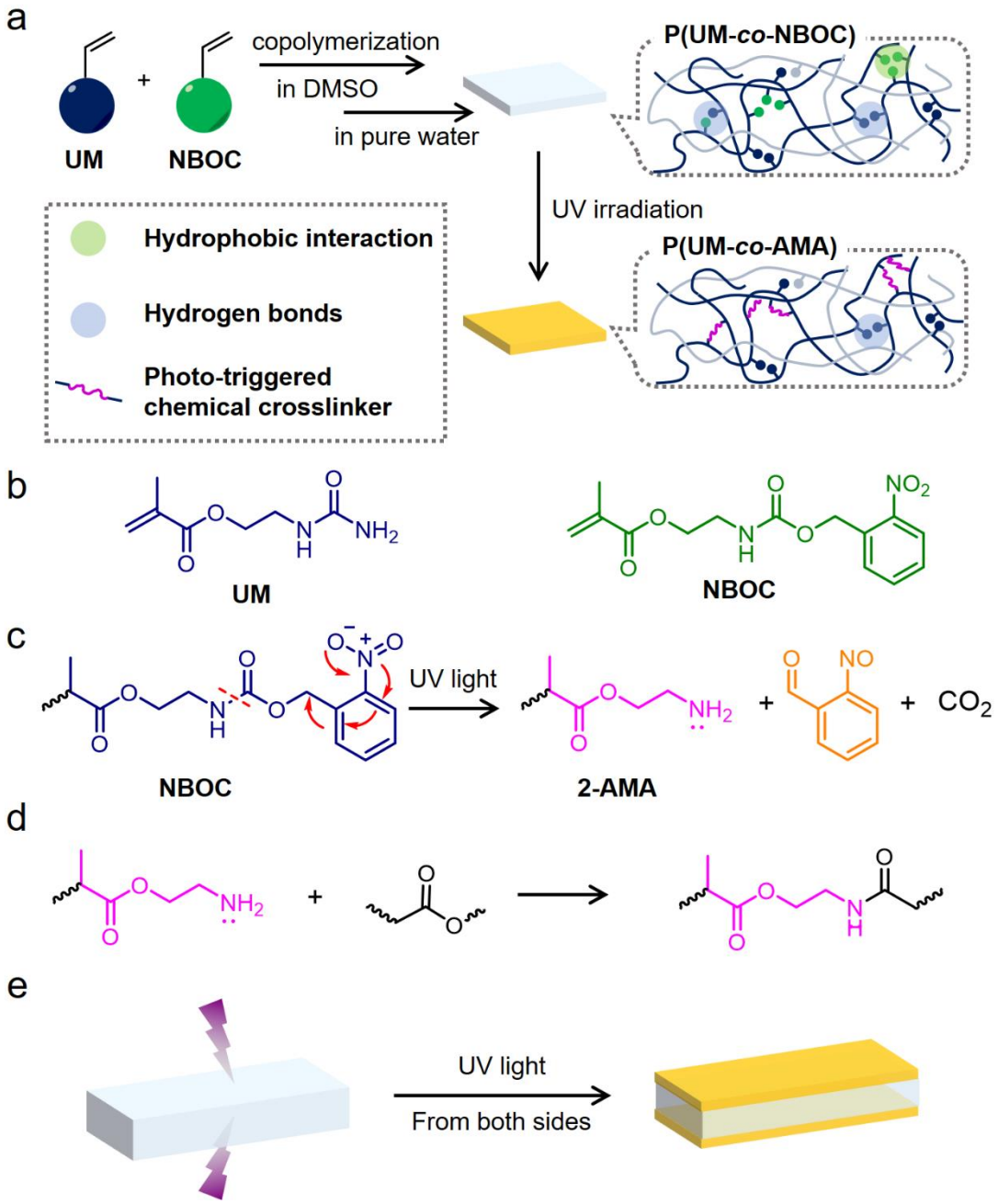


Figure 4.1 (a) Synthesis routine of P(UM-co-NBOC) hydrogels and the P(UM-co-AMA) hydrogels; (b) Chemical structure of starting monomers; (c) Photo-triggered self-immolative reaction; (d) Subsequent chemical crosslinking following self-immolative reaction; (e) Schematic illustration of fabrication of hydrogel composites with sandwich structure.

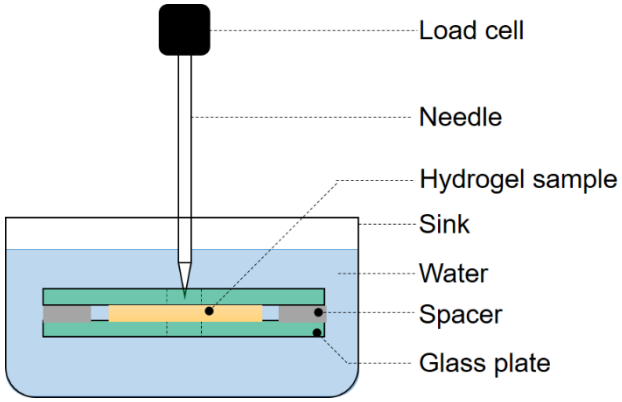


Figure 4.2 Schematic illustration of the puncture test.

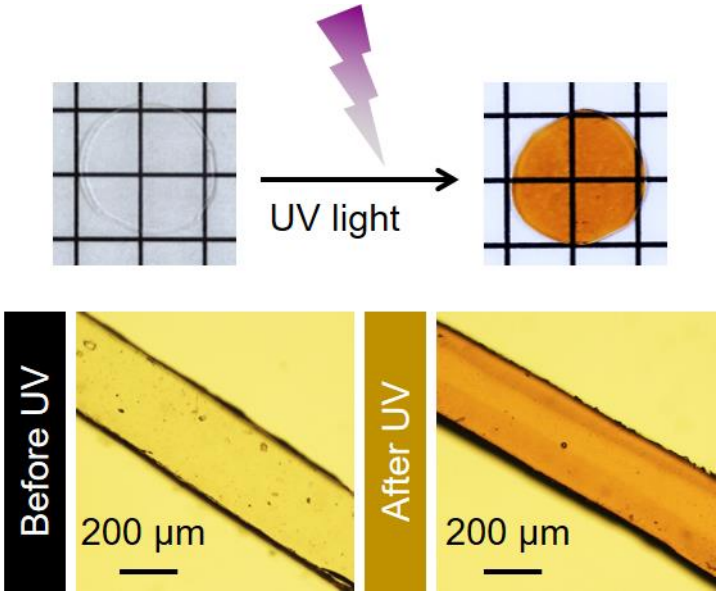


Figure 4.3. Photos and cross-section micrograph of hydrogel before and after UV irradiation.

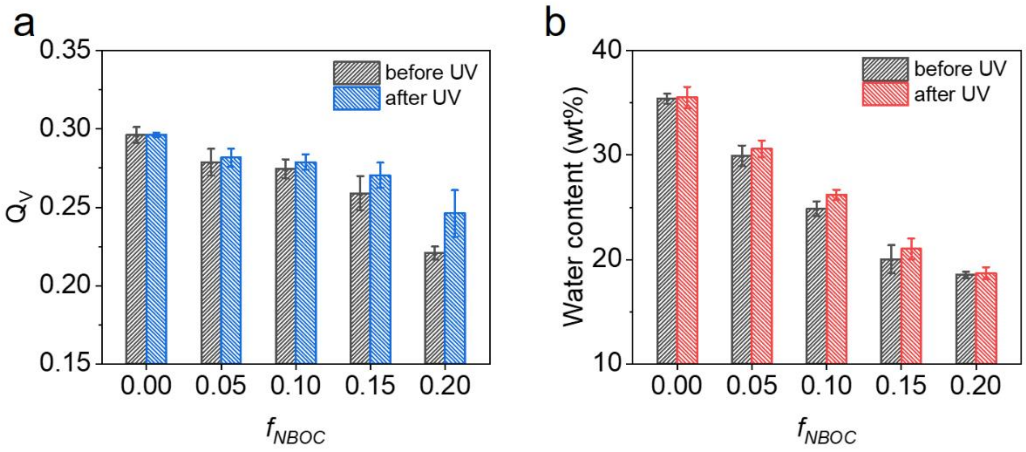


Figure 4.4. Q_V (a) and changes in water content (b) of P(UM-*co*-NBOC) before and after UV irradiation.

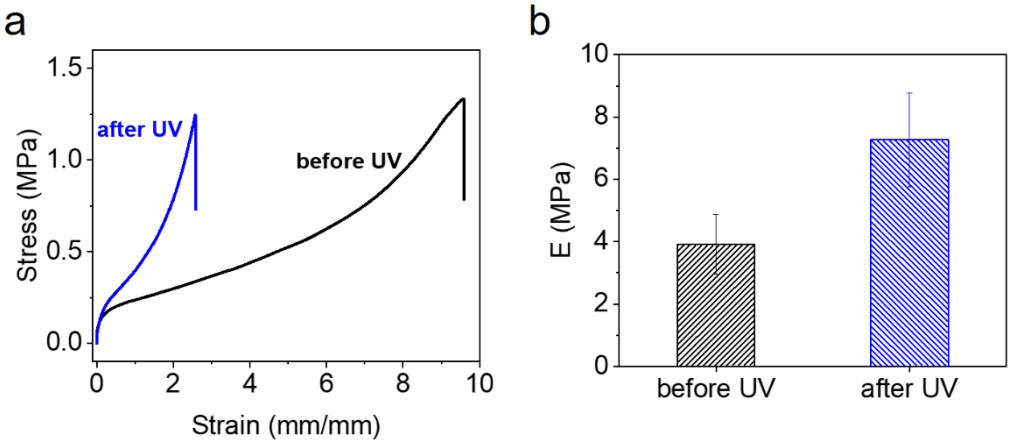


Figure 4.5 Contrast of tensile stress-strain curve (a) and Young's modulus (b) of hydrogels before and after UV irradiation.

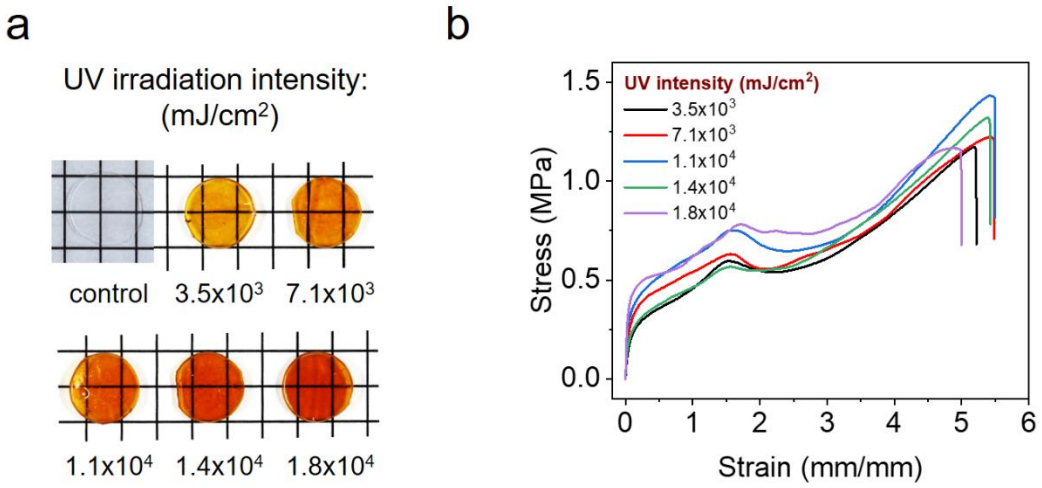


Figure 4.6 Photography (a) and tensile test (b) of hydrogels after UV irradiation with varied UV intensity.

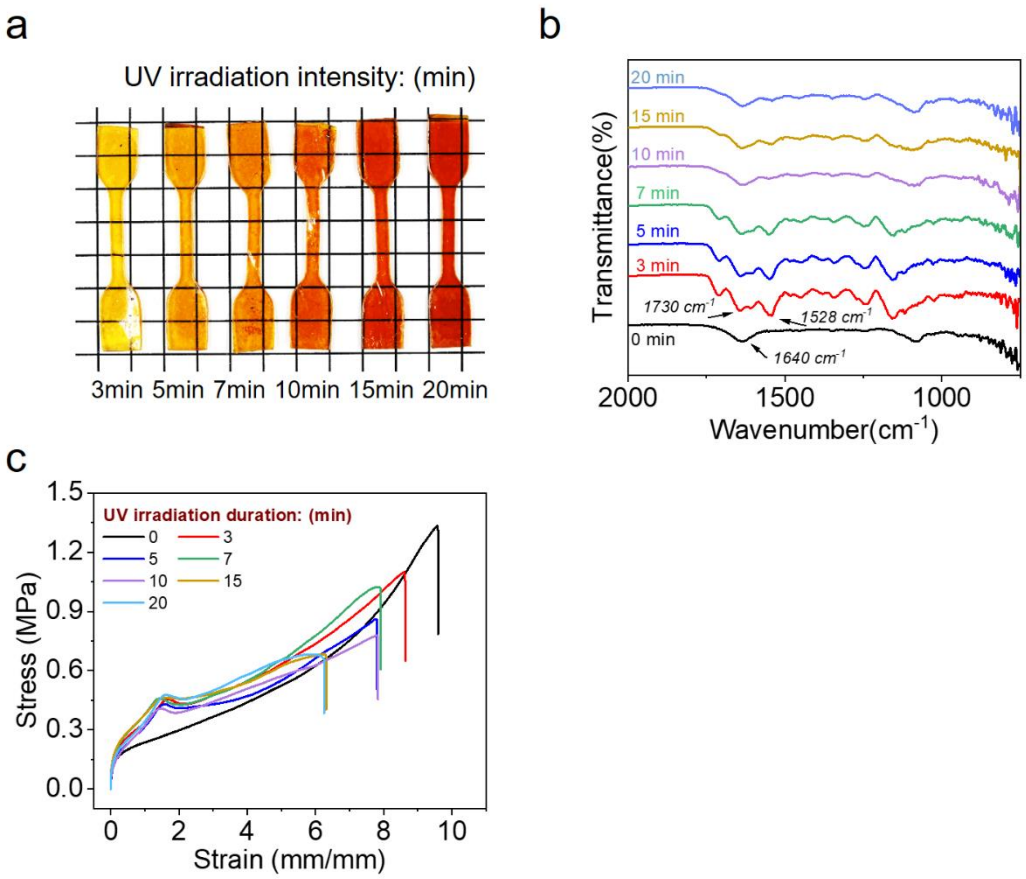


Figure 4.7 Photography (a) and FTIR spectra (b) of P(UM-*co*-AMA) in sandwich hydrogels (f_{NBOC} 0.15) over varied UV duration; (c) Tensile test of P(UM-*co*-AMA) in sandwich hydrogels (f_{NBOC} 0.15) over varied UV duration.

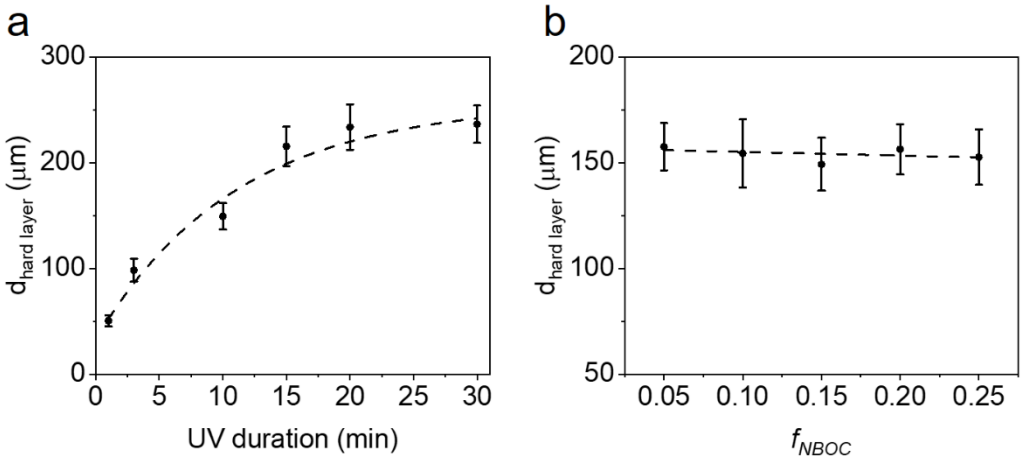


Figure 4.8 (c) Dependence of thickness of P(UM-*co*-AMA) in sandwich hydrogels (f_{NBOC} 0.15) on UV duration; (b) Changes in the thickness of P(UM-*co*-AMA) in sandwich hydrogels with different f_{NBOC}.

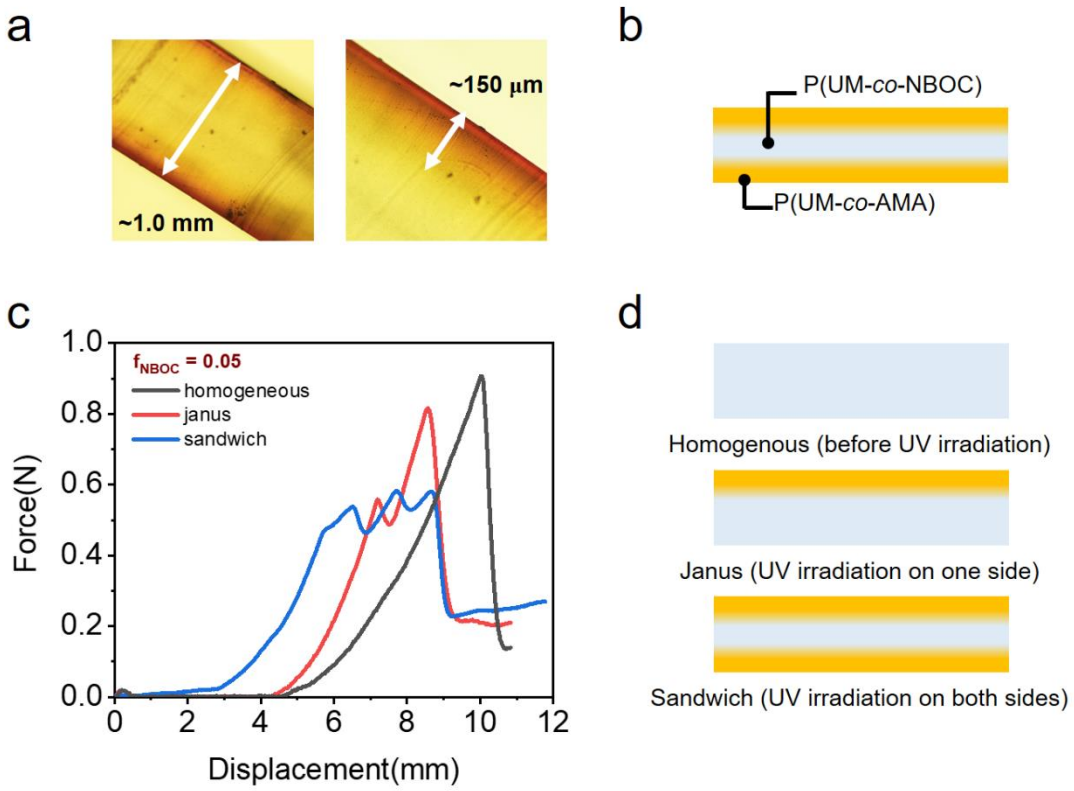


Figure 4.9 P(UM-*co*-NBOC) hydrogels with hieratical structure after UV irradiation. Cross-section micrograph (a) and scheme of P(UM-*co*-NBOC) hydrogels with sandwich-like structure upon UV irradiation; puncture test (c) and scheme (d) for P(UM-*co*-NBOC)-0.05 hydrogels with hieratical structures.

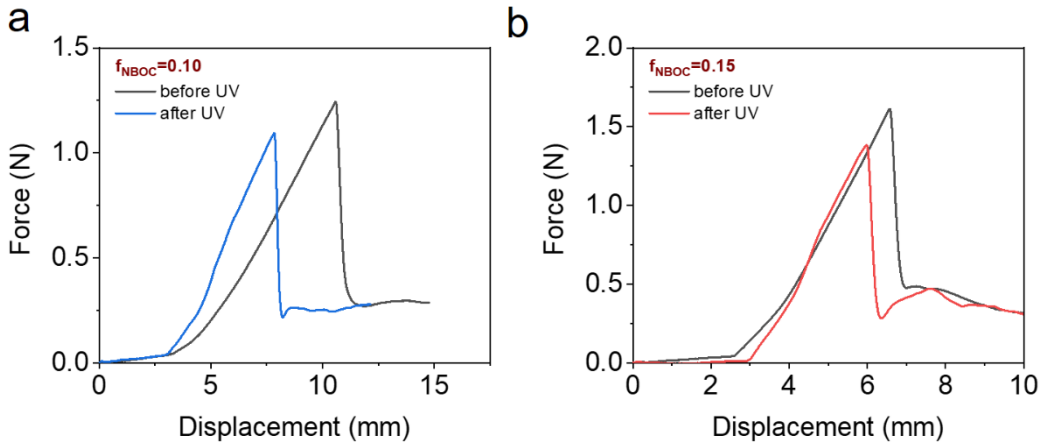


Figure 4.10 Puncture test for P(UM-*co*-NBOC)-0.1 (a) and P(UM-*co*-NBOC)-0.15 (b) hydrogels.

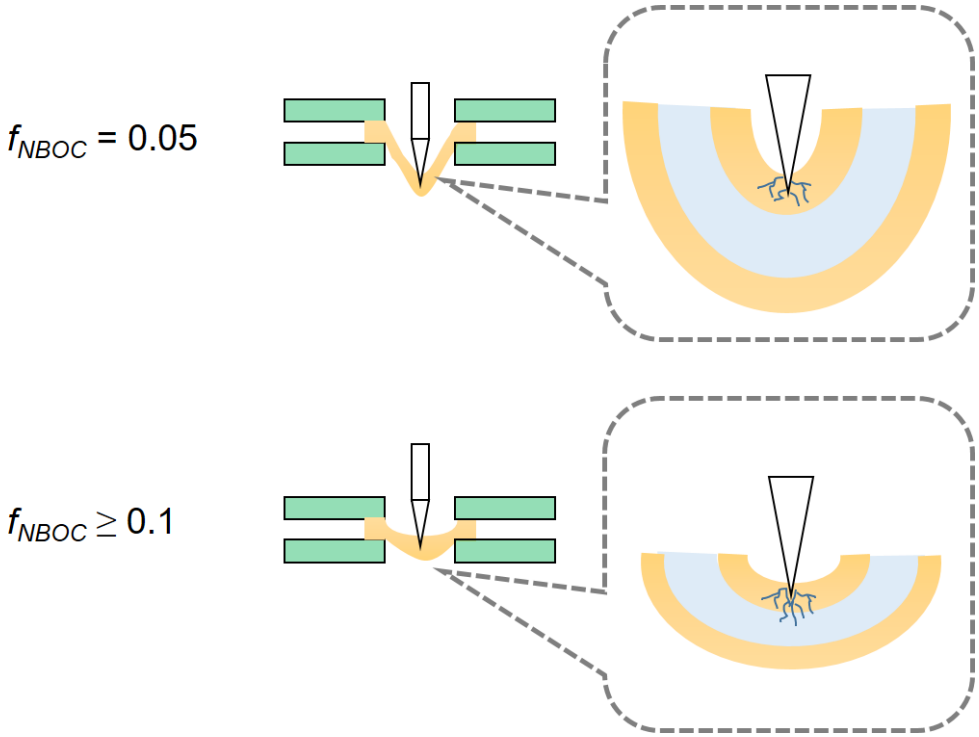


Figure 4.11 Schematic illustration of the hypothesis for puncture tests of sandwich hydrogels with different f_{NBOC}.

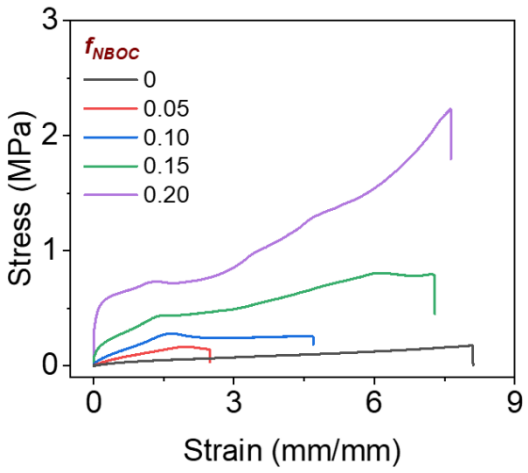


Figure 4.12 Tensile test of sandwich hydrogels after UV irradiation with different f_{NBOC}.

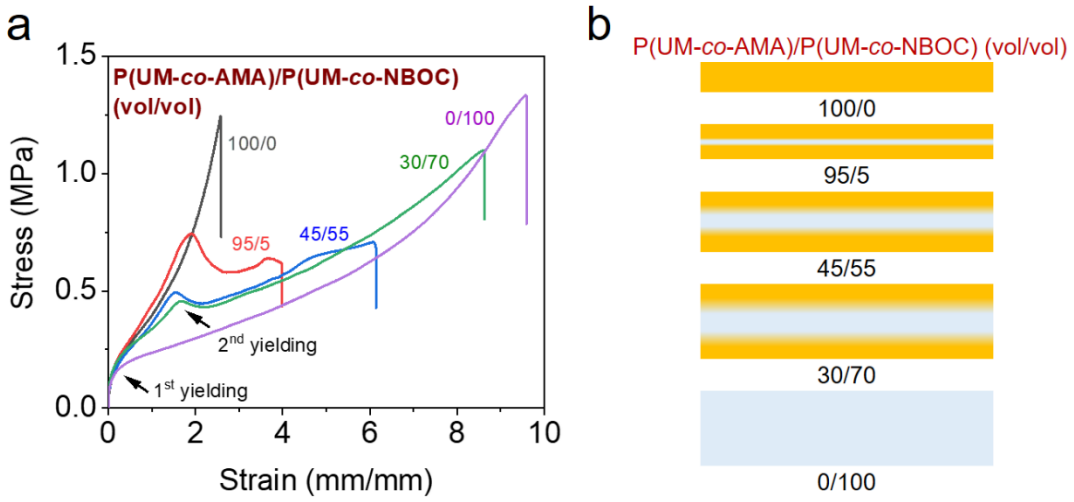


Figure 4.13 Tensile test (a) and scheme (b) for P(UM-*co*-NBOC)-0.15 hydrogels with different P(UM-*co*-AMA)/P(UM-*co*-NBOC) ratio (vol/vol).

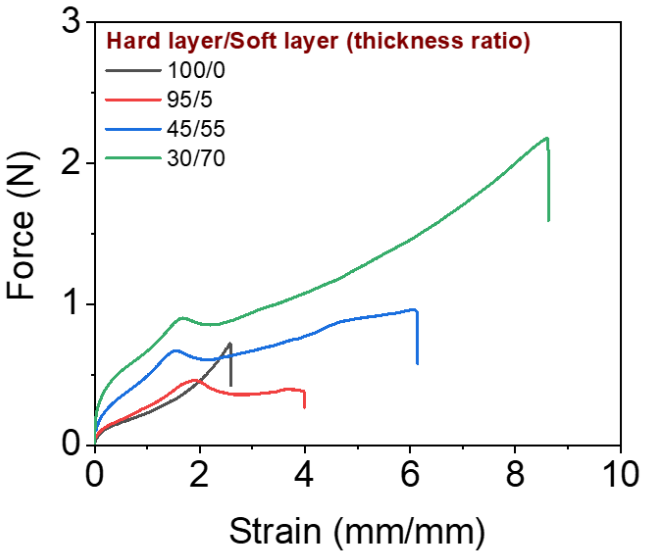


Figure 4.14 Tensile force-strain curves of the composite hydrogels with sandwiched layer structure with different layer thickness ratio. The ratio was varied by UV irradiation to P(UM-*co*-NBOC)-0.15 hydrogels of different thickness from both sides of the sample. Each outer layer thickness was kept constant at 150 μm while the middle layer thickness changes as shown in **Figure 4.8**.

.

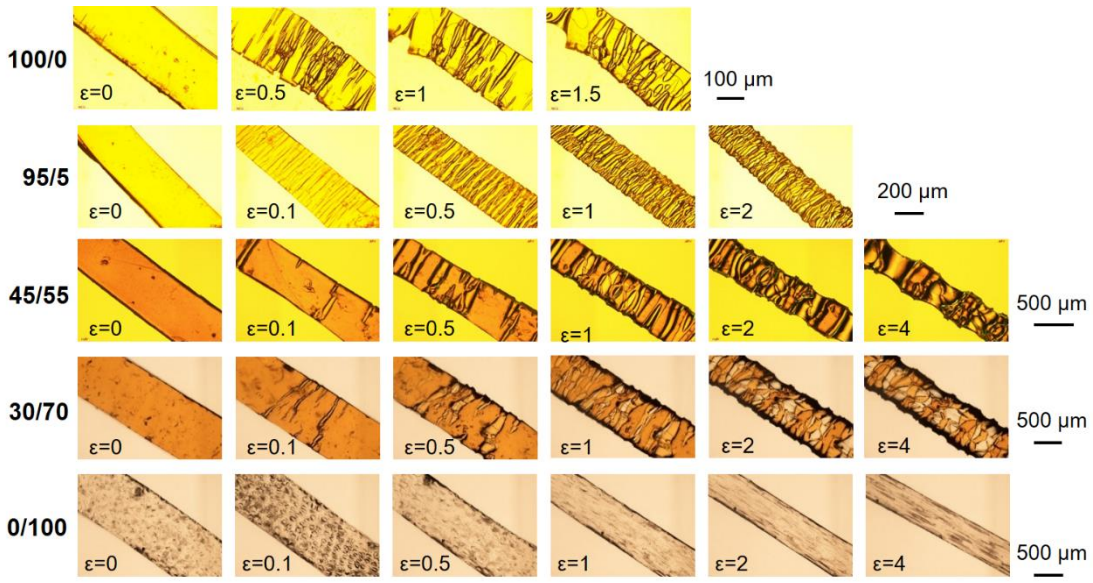


Figure 4.15 The composite hydrogels with sandwiched layer structure composed of hard outer layers of P(UM-*co*-AMA) hydrogel and soft middle hydrogel of P(UM-*co*-NBOC) gel. Optical microscope images of the sandwich hydrogel under stretching at different strains. The small drops on the surface of pristine P(UM-*co*-NBOC) gel (0/100) at strain 0.1 were water drops placed on the gel surface to prevent drying.

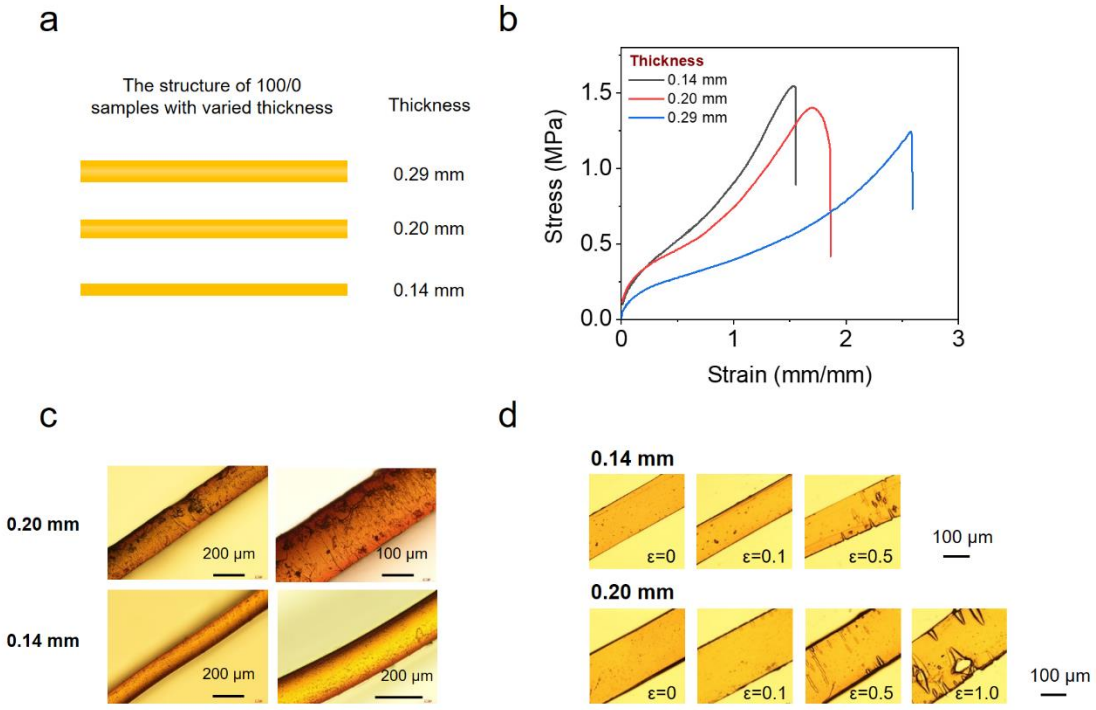


Figure 4.16 The 100/0 samples with different thickness. (a) Structure scheme, (b) tensile stress-strain curves of samples with different thickness. (c) Optical microscope images. (d) Optical microscope images of the 100/0 hydrogel under stretching at different strains.

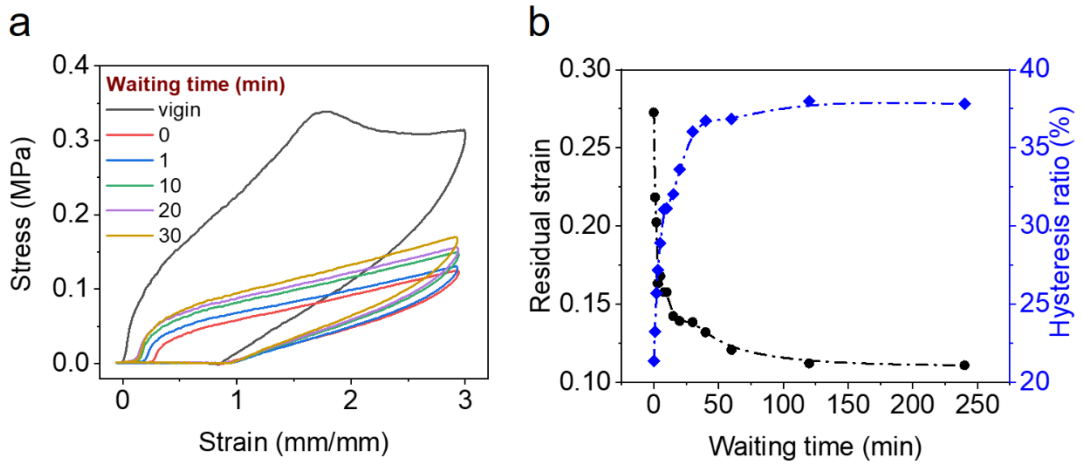


Figure 4.17 Self-recovery behaviors of the sandwich hydrogel (30/70). (a) Cyclic loading-unloading curves, and (b) residual strain and hysteresis recovery ratio between the second and first loading cycles for different waiting times.

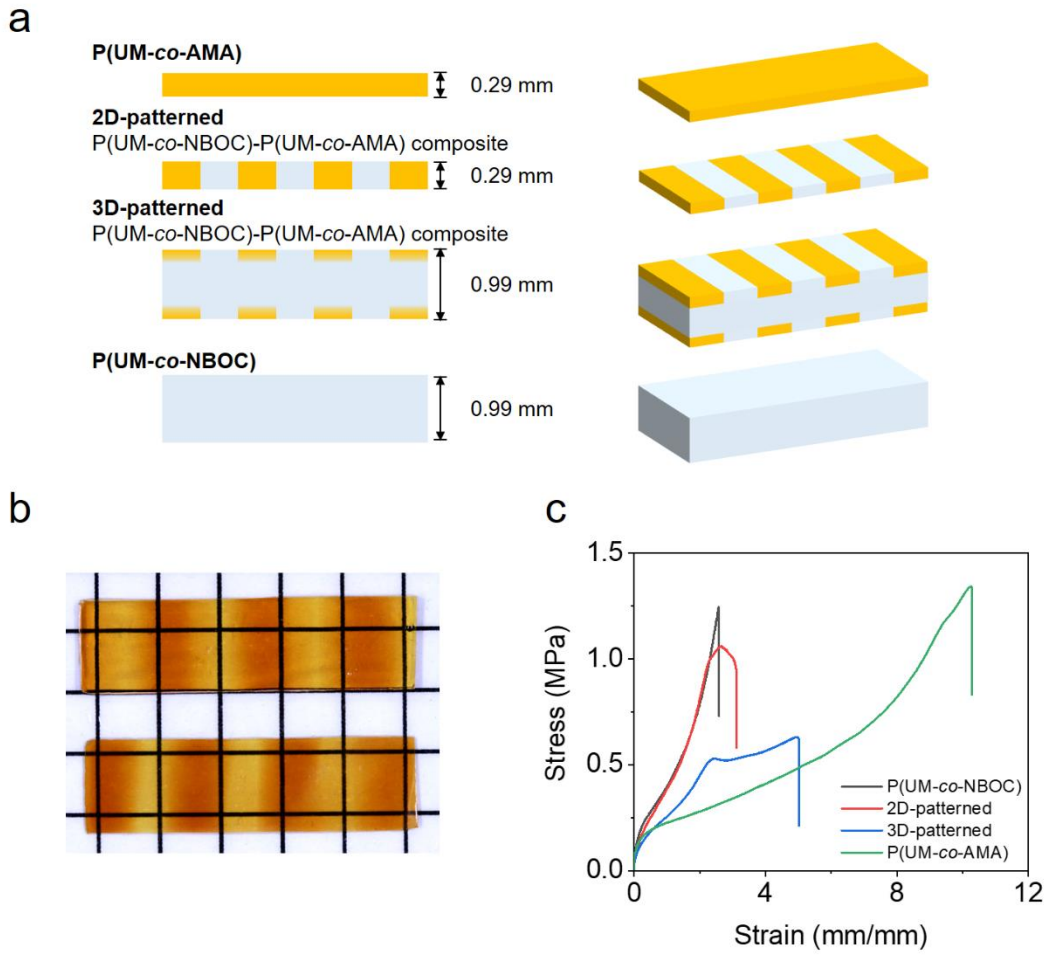


Figure 4.18 (a) Scheme for the cross-section and (b) photos of the composites and (c) comparison between mechanical properties of different hydrogels and their 2D and 3D patterned composites. The pristine gel was P(UM-*co*-NBOC)-0.15. The UV was irradiated from both sides of the sample. After UV irradiation, the 3D-patterned hydrogel composite formed a sandwiched structure with two outer layers of hard and soft strip patterns and one soft middle layer, with thickness ratio 30/70. The width of the alternating strips was 3 mm.

Chapter 5

Hydrogel composites based on photo-responsive P(HEA-*co*-NBOC) copolymer

5.1 Introduction

To mimic the stimuli-responsive behavior in natural hydrogels, synthetic polymers materials performing similar attributes have been widely developed as well.[1] For stimuli-responsive hydrogels, their structure,[2, 3] such as the crosslinkers or the chain entanglements, or properties, such as wettability[4] or adhesion,[5] could adapt to surrounding environment upon exposure to a stimulus, namely, photo,[4, 5] electrochemical,[6] and pH,[7] etc.

Light stimulation is particularly interesting for many applications because of the capability of contact-free remote manipulation and inherent spatial and temporal control[8]. Moreover, light can be finely adjusted in its intrinsic properties, such as wavelength and intensity[9, 10]. Therefore, the photo-responsive hydrogels could be taken as ideal candidates in several fields, including biomedical device[11, 12], adaptive surface[13, 14], soft robots[15] and etc.

In this work, we synthesized copolymers from hydrophilic 2-ureidoethyl methacrylate (UM) and hydrophobic photo-responsive (2-nitrobenzyloxycarbonylaminoethyl

methacrylate, NBOC) (**Chapter 4**). The NBOC residues in the P(UM-co-NBOC) copolymers play two roles. One is working as physical crosslinkers based on their hydrophobic association, which can dissipate a large amount of energy during deformation so that toughen the hydrogels; the other is providing photo-responsiveness to switch the physical crosslinking to chemical crosslinking[16]. That work provides a new strategy to fabrication tough hydrogel composites by incorporating a photo-responsive hydrophobic residue into the hydrogel network. To test the universality of the function of NBOC in the network, we further copolymerized NBOC with 2-hydroxyethyl acrylate (HEA) monomer, which has no strong physical interactions between HEA monomers (**Figure 5.1**).

5.2 Experimental

5.2.1 Materials

2-Nitrobenzyloxycarbonylaminoethyl methacrylate (NBOC) was synthesized according to literature.[16] 2-hydroxyethyl acrylate (HEA) were provided by Osaka chemicals Co., Ltd. 2,2′-Azobisisobutyronitrile (AIBN, 98%) was purchased from Sigma-Aldrich. N,N’-methylenebis (acrylamide) (MBAA) was purchased from Tokyo Kasei Co., Ltd. Dimethyl sulfoxide (DMSO) was purchased from Wako Pure Chemical Industries, Ltd. All chemicals were used as received.

5.2.2 Synthesis of hydrogels

The monomers with different monomer molar ratios were first dissolved in their co-solvent DMSO. The pre-gel solution contains 1.5 M HEA and NBOC, 0.0015 M MBAA (chemical cross-linker) and 0.003 M AIBN.

The pre-gel solution was then poured into in a reaction cell consisting of a pair of glass plates with a spacer, and heated at 70 ℃ for 8 hours. After polymerization, the as-prepared gel was immersed in a large amount of water for 1 week to reach equilibrium. The hydrogels were named as polymer-f_{NBOC}, where f_{NBOC} was the molar fraction of NBOC.

5.2.3 Characterization of hydrogels

Swelling measurements

The as-prepared gel was cut into samples with fixed sizes and then immersed in a large amount of pure water until reaching equilibrium. The swelling volume ratio Q_v was defined as the ratio of the sample volume at swelling equilibrium V to that in the as-prepared state V_0, $Q_v = V/V_0$.

Water content

The water content (W_{water}, wt%) of hydrogel samples was measured with a moisture balance (MOC-120H, SHIMADZU Co., Japan) based on the equation, $W_{water} = (m_{water}/m_{sample}) *100\%$, where m_{water} *(g)* is the weight of water in the hydrogel network, and m_{sample} *(g)* is the weight of the whole hydrogel sample.

Mechanical test

Uniaxial tensile tests were performed on hydrogels using a tensile-compressive tester (Instron 5965 type universal testing system) in air. The cyclic tensile stress-strain measurements were performed using a tensile-compressive tester (Tensilon RTC-1310A, Orientec Co.) in a water bath to prevent water from evaporating from the samples. The dissipated energy, calculated by the hysteresis area (U_{hys}), and the hysteresis coefficient, the ratio of hysteresis area to the overall area below the loading curve, was named as U_{hys} coefficient.

All tests were carried out on dumbbell-shaped samples with the standard JIS-K6251-7 size (12 mm (L) × 2 mm (d) × 0.3–3 mm (w)). All samples were stretched along the length direction of the samples at a deformation rate of 100 mm/min.

UV irradiation

UV irradiation on samples was conducted on a UV-LED irradiation panel (UAW365-31110-1212F, Sentech Co.). The intensity of UV irradiation is 1.78×10^4 mJ/cm^2. The hydrogel samples were immersed in a cell of DI water to prevent water from

evaporating from the samples during irradiation. And the cell consists of a pair of glass plates with a spacer.

5.3 Results and discussion

5.3.1 before UV irradiation

We conducted the copolymerization of HEA and NBOC as follows: first dissolve hydrophobic NBOC and hydrophilic monomer into their co-solvent DMSO, and performed random radical polymerization at high monomer concentration so that the polymers formed are well above their entanglement concentration to obtain organogel. Since no strong physical interactions between HEA monomers (Figure 4.1). In P(HEA-*co*-NBOC) system, we add a small amount of MBAA to chemically crosslink the polymer network, otherwise, no gel would be formed. Thus, we introduced NBOC into chemical crosslinked hydrophilic network, by means of copolymerization of hydrophobic NBOC with HEA.

During the solution replacement process, the NBOC residues aggregate into hydrophobic domain working as physical crosslinks. In the solvent exchange process, the P(HEA-*co*-NBOC) gel with low f_{NBOC} (< 0.05) swelled due to its high hydrophilicity of polymer chains. When the f_{NBOC} is larger than 0.05, the gel became shrink due to the formation of sufficient hydrophobic physical crosslinks, resulting in low water content

(**Figure 5.2**).

The formation of physical crosslinkers by hydrophobic interaction between NBOC residues significantly enhances the mechanical properties of hydrogel (**Figure 5.1**). The mechanic test shows that introducing NBOC can enhance the mechanical properties of hydrogel dramatically. With the increase of f_{NBOC}, fracture stress, fracture strain, Young's modulus, and toughness increased dramatically (**Figure 5.3**). Addition of f_{NBOC} as small as 0.03, resulted into 1.8 times of fracture stress and strain, and double times of Young's modulus and toughness when compared to pure PHEA hydrogels. Distinct yielding coming from physical crosslinkers could be easily observed in tensile curve of P(HEA-*co*-NBOC)-0.1 hydrogel, which was resulted from the increasing of reversible physical crosslinkers.

To further investigate the hydrogels reinforced by hydrophobic interaction, loading-unloading tests were conducted to evaluate the hysteresis and energy dissipation of hydrogels (**Figure 5.4**). Distinct yielding and hysteresis were observed in the loading-unloading cycle of hydrogels. U_{hys} and U_{hys} coefficient increased with the f_{NBOC} in P(HEA-*co*-NBOC) hydrogels (**Figure 5.4**). It indicates that the energy used for deformation could be dissipated by breaking of the hydrophobic interaction. U_{hys} of pure PHEA was 0.9 kJ/m^3 with corresponding U_{hys}/W_{max} of 11% and the U_{hys} of P(HEA-*co*-NBOC)-0.1 was 12.8 kJ/m^3 with corresponding U_{hys}/W_{max} of 50%, which elevated around 15 times (**Figure 5.4**).

The detached physical crosslinkers, by which energy can be dissipated during

deformation of hydrogel samples, will reconstruct subsequently. Thus, the dynamic and reversible feature of physical crosslinkers endowed the hydrogel with good self-recovery behavior and fatigue resistance. Cyclic loading-unloading tensile tests were performed to investigate the self-recovery ability of P(HEA-*co*-NBOC) hydrogels (**Figure 5.5**). P(HEA-co-NBOC)-0.1 hydrogels were chosen as representative, because of their outstanding U_{hys} and U_{hys} coefficient of first loading-unloading cycle.

The dependence of recovery on waiting time and two-stage recovery process could also be observed in P(HEA-*co*-NBOC)-0.1 hydrogel (**Figure 5.5**). However, after 2 hours, hysteresis ratio could not reach to 100% of original state. Meanwhile, the hydrogel exhibited constant residual strain around 0.1 even the deformation (strain = 300%) relative to fracture strain (strain = 2700%) was so small. Contrast with complete self-recovery of P(UM-*co*-NBOC)-0.15 hydrogel, the partial self-recovery of P(HEA-*co*-NBOC)-0.1 hydrogel was supposed to be resulted from the irreversible breakage of chemical crosslinkers.

5.3.2 After UV irradiation

Upon UV irradiation, the 2-nitrobenzyl function group of NBOC exhibits photo-labile characteristics, with the release of 2-nitrobenzaldehyde and CO_2, as shown in **Figure 5.1**. The resultant amino groups would further attack other ester bonds to generate new chemical crosslinkers.

Due to the color of by-product of 2-nitrobenzaldehyde, the hydrogel turned yellow after UV irradiation. After hydrogel reaching equilibrium in DI water, there was no significant change in volume of hydrogels before and after UV irradiation (**Figure 5.6**). Upon UV irradiation, the hydrophobic NBOC transforms into hydrophilic moieties by self-immolative reaction firstly, which induces the disassembly of physical crosslinkers composed of hydrophobic interaction, subsequently followed by generation of new chemical crosslinkers between amino groups and ester bondings (**Figure 5.1**). The slight difference in water content and Q_v, infecting the slight change in total amount of crosslinkers. Thus, the physical crosslinkers composed of hydrophobic interaction between NBOC damaged by the UV irradiation, are supposed to be just replaced by the newly formed chemical crosslinkers.

After UV irradiation, the P(HEA-*co*-NBOC) hydrogel can convert to P(HEA-*co*-AMA) hydrogel as well. Figure 6d shows the stress-strain curves of sandwich-like P(HEA-*co*-NBOC)-P(HEA-*co*-AMA) hydrogel (f_{NBOC} 0.1) and its pure P(HEA-*co*-NBOC) hydrogel before UV irradiation. The sandwich hydrogel, which network sacrificed partial reversible physical bonds by forming covalent bonds, present higher Young's modulus but shorter fracture strain. The gel also shows a special yielding phenomenon in the tensile curve (**Figure 5.7**). **Figure 5.8** showed the tensile process of sandwich hydrogel: the yellow surface broke at the beginning of deformation, then the matrix performed homogeneous deformation after fragmentation of surface, which was very similar with UM-based sandwich hydrogels. However, the new yielding was quite

different from that in UM-based sandwich hydrogel, but very similar with the macroscale composite hydrogels reported by our group before[17, 18]. It was supposed to be attributed to the dramatic difference between the strength of P(HEA-*co*-AMA) and P(HEA-*co*-NBOC). P(HEA-*co*-NBOC), which was generated upon UV irradiation, was so brittle that the polymeric network could not keep continuous after fragmentation of surface, which was composed of (HEA-*co*-AMA).

The P(HEA-*co*-NBOC) hydrogel can also be patterned by using a mask under UV irradiation. However, different from UM-based 3D-pattern gel, HEA-based 3D-pattern hydrogel shows ununiformed shape at equilibrium state, due to unmatched swelling behaviors of two components (**Figure 5.9**). Therefore, combining UV irradiation and mismatched swelling behavior, HEA-based hydrogel shows great candidate as matrix hydrogel for the construction of more complicated hieratical materials.

5.4 Conclusion

Based on addition of hydrophobic interaction by copolymerization with NBOC, mechanical properties, toughness and fatigue resistance of P(HEA-*co*-NBOC) hydrogels improved dramatically. After UV irradiation, part of physical crosslinkers composed of hydrophobic interaction transformed into chemical crosslinkers, new surface generated with instinctive mechanical properties. The hydrogels upon UV irradiation showed different Young's modulus. Thus, composite hydrogels based on

copolymerization of photo-responsive, NBOC, and hydrophilic monomers, could be easily prepared *in situ* by UV irradiation. And their structure and properties could be modulated by thickness, f_{NBOC} and duration of UV irradiation.

Reference

1. Stuart, M. A.; Huck, W. T.; Genzer, J.; Muller, M.; Ober, C.; Stamm, M.; Sukhorukov, G. B.; Szleifer, I.; Tsukruk, V. V.; Urban, M.; Winnik, F.; Zauscher, S.; Luzinov, I.; Minko, S., Emerging applications of stimuli-responsive polymer materials. *Nat Mater* **2010,** *9* (2), 101-13.

2. Matsuda, T.; Kawakami, R.; Namba, R.; Nakajima, T.; Gong, J. P., Mechanoresponsive self-growing hydrogels inspired by muscle training. *Science* **2019,** *363* (6426), 504-508.

3. Masuda, T.; Ueki, T.; Tamate, R.; Matsukawa, K.; Yoshida, R., Chemomechanical Motion of a Self-Oscillating Gel in a Protic Ionic Liquid. *Angew Chem Int Ed Engl* **2018,** *57* (51), 16693-16697.

4. Huang, X.; Sun, Y.; Soh, S., Stimuli-Responsive Surfaces for Tunable and Reversible Control of Wettability. *Adv Mater* **2015,** *27* (27), 4062-8.

5. Gao, Y.; Wu, K.; Suo, Z., Photodetachable Adhesion. *Adv Mater* **2019,** *31* (6), e1806948.

6. Palleau, E.; Morales, D.; Dickey, M. D.; Velev, O. D., Reversible patterning and actuation of hydrogels by electrically assisted ionoprinting. *Nat Commun* **2013,** *4*, 2257.

7. Kureha, T.; Aoki, D.; Hiroshige, S.; Iijima, K.; Aoki, D.; Takata, T.; Suzuki, D., Decoupled Thermo- and pH-Responsive Hydrogel Microspheres Cross-Linked by Rotaxane Networks. *Angew Chem Int Ed Engl* **2017,** *56* (48), 15393-15396.

8. Li, L.; Scheiger, J. M.; Levkin, P. A., Design and Applications of Photoresponsive Hydrogels. *Adv Mater* **2019,** *31* (26), e1807333.

9. Maity, C.; Hendriksen, W. E.; van Esch, J. H.; Eelkema, R., Spatial structuring of a supramolecular hydrogel by using a visible-light triggered catalyst. *Angew Chem Int Ed Engl* **2015,** *54* (3), 998-1001.

10. Zhou, H.; Xue, C.; Weis, P.; Suzuki, Y.; Huang, S.; Koynov, K.; Auernhammer, G. K.; Berger, R.; Butt, H. J.; Wu, S., Photoswitching of glass transition temperatures of azobenzene-containing polymers induces reversible solid-to-liquid transitions. *Nat Chem* **2017,** *9* (2), 145-151.

11. Luo, Y.; Shoichet, M. S., A photolabile hydrogel for guided three-dimensional cell growth and migration. *Nat Mater* **2004,** *3* (4), 249-53.

12. Lee, T. T.; Garcia, J. R.; Paez, J. I.; Singh, A.; Phelps, E. A.; Weis, S.; Shafiq, Z.; Shekaran, A.; Del Campo, A.; Garcia, A. J., Light-triggered in vivo activation of adhesive peptides regulates cell adhesion, inflammation and vascularization of biomaterials. *Nat Mater* **2015,** *14* (3), 352-60.

13. Yoon, J.; Bian, P.; Kim, J.; McCarthy, T. J.; Hayward, R. C., Local switching of chemical patterns through light-triggered unfolding of creased hydrogel surfaces. *Angew Chem Int Ed Engl* **2012,** *51* (29), 7146-9.

14. Ming, Z.; Ruan, X.; Bao, C.; Lin, Q.; Yang, Y.; Zhu, L., Micropatterned Protein for Cell Adhesion through Phototriggered Charge Change in a Polyvinylpyrrolidone Hydrogel. *Advanced Functional Materials* **2017,** *27* (25).

15. Chen, J.; Leung, F. K.; Stuart, M. C. A.; Kajitani, T.; Fukushima, T.; van der Giessen, E.; Feringa, B. L., Artificial muscle-like function from hierarchical supramolecular assembly of photoresponsive molecular motors. *Nat Chem* **2018,** *10* (2), 132-138.

16. Wang, X.; Liu, G.; Hu, J.; Zhang, G.; Liu, S., Concurrent block copolymer polymersome stabilization and bilayer permeabilization by stimuli-regulated "traceless" crosslinking. *Angew Chem Int Ed Engl* **2014,** *53* (12), 3138-42.

17. Takahashi, R.; Sun, T. L.; Saruwatari, Y.; Kurokawa, T.; King, D. R.; Gong, J. P., Creating Stiff, Tough, and Functional Hydrogel Composites with Low-Melting-Point Alloys. *Adv Mater* **2018,** *30* (16), e1706885.

18. Huang, Y.; King, D. R.; Sun, T. L.; Nonoyama, T.; Kurokawa, T.;

Nakajima, T.; Gong, J. P., Energy-Dissipative Matrices Enable Synergistic Toughening in Fiber Reinforced Soft Composites. *Advanced Functional Materials* **2017,** *27* (9).

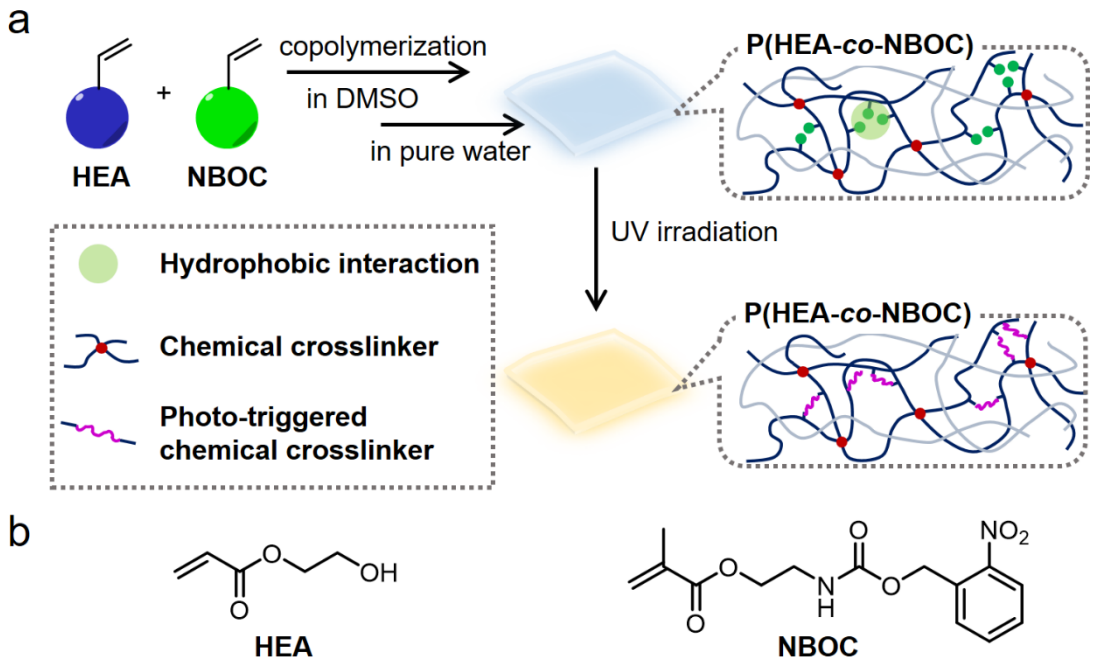


Figure 5.1 (a) Synthesis routine of P(HEA-*co*-NBOC) hydrogel; (b) chemical structure

of monomers.

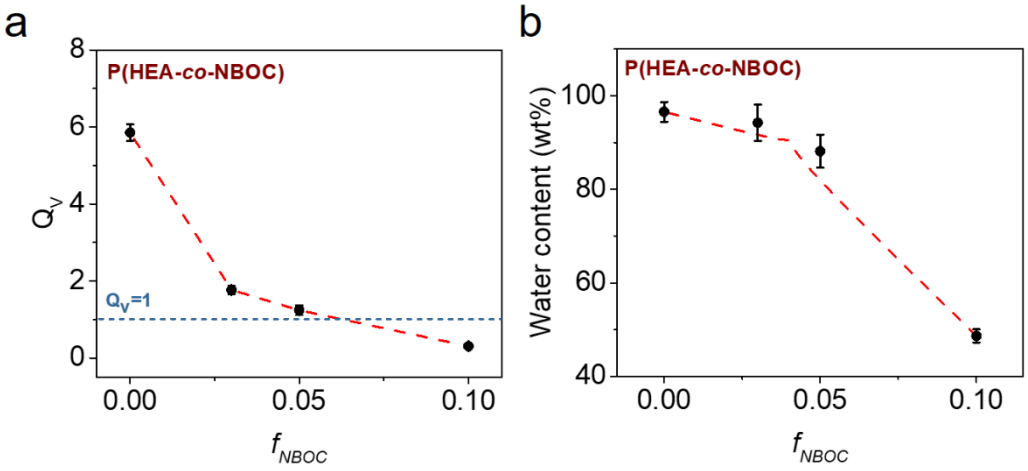


Figure 5.2 Q_V (a) and water content (b) of P(HEA-*co*-NBOC) hydrogel with different f_{NBOC}.

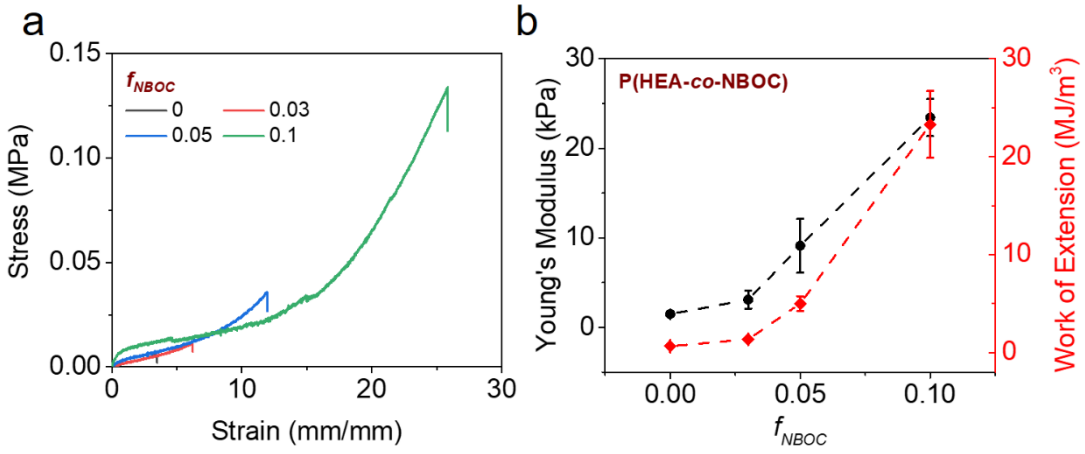


Figure 5.3 Tensile stress-strain curves and mechanical strength values of hydrogels with different f_{NBOC}. (a, b) P(HEA-*co*-NBOC).

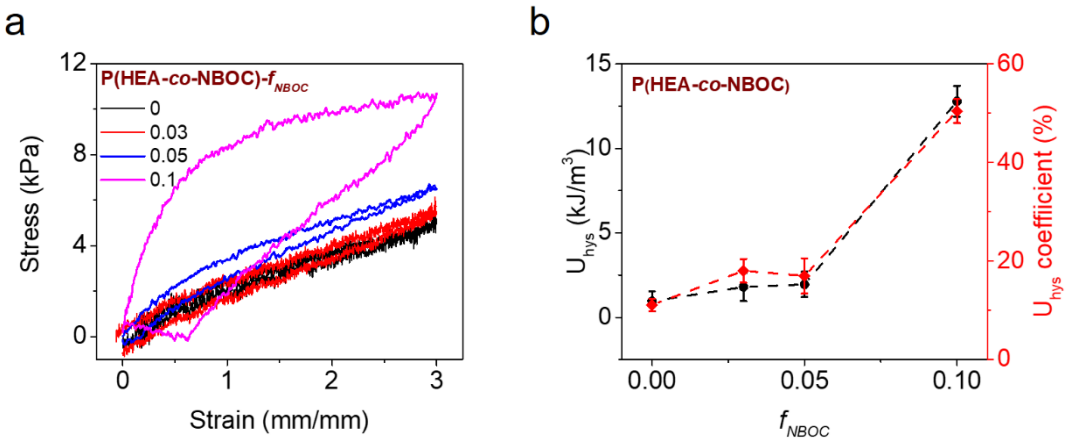


Figure 5.4 Loading-unloading tests, the calculated dissipated energy and energy dissipation coefficient of hydrogels P(HEA-*co*-NBOC) (a, b).

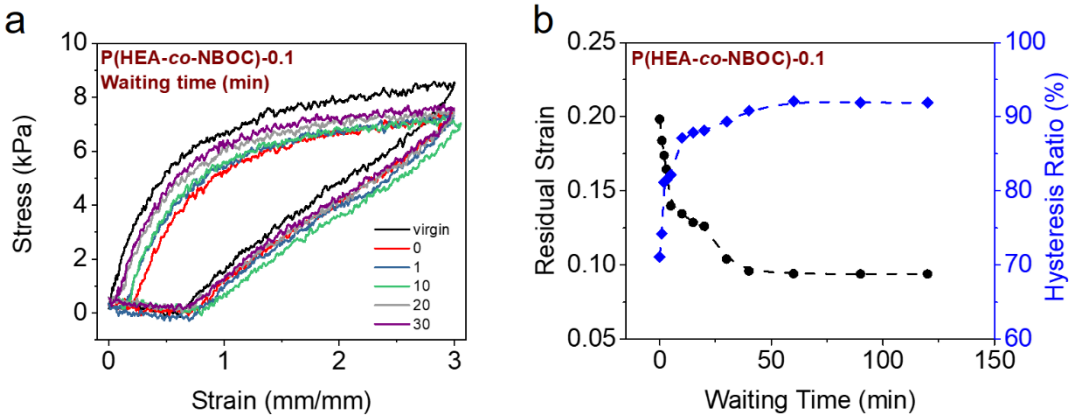


Figure 5.5 Cyclic loading-unloading curves, residual strain and hysteresis ratio of hydrogels P(HEA-*co*-NBOC)-0.1 (a, b) with different f_{NBOC}.

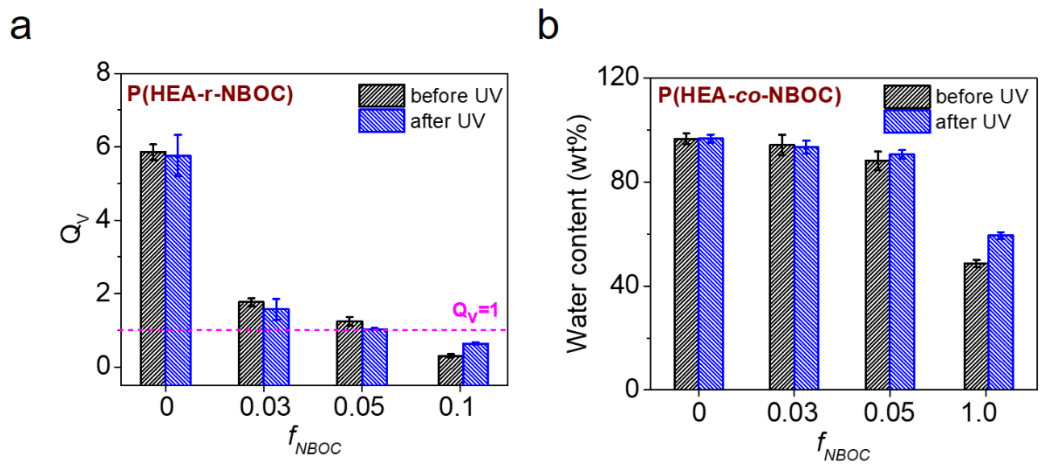


Figure 5.6 Changes in Q_V (a) and water content (b) of P(HEA-*co*-NBOC) before and after UV irradiation.

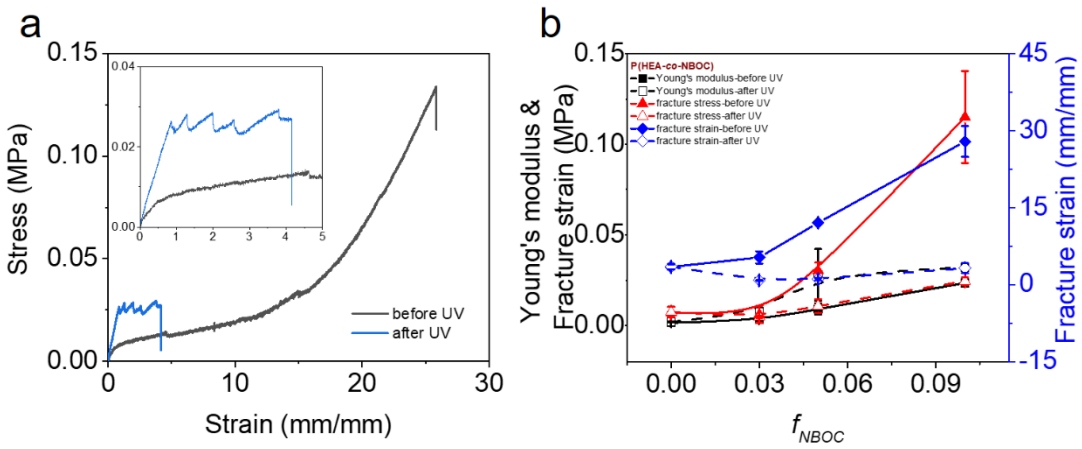


Figure 5.7 Contrast of mechanical properties of P(HEA-*co*-NBOC)-0.1 hydrogel before and after UV irradiation.

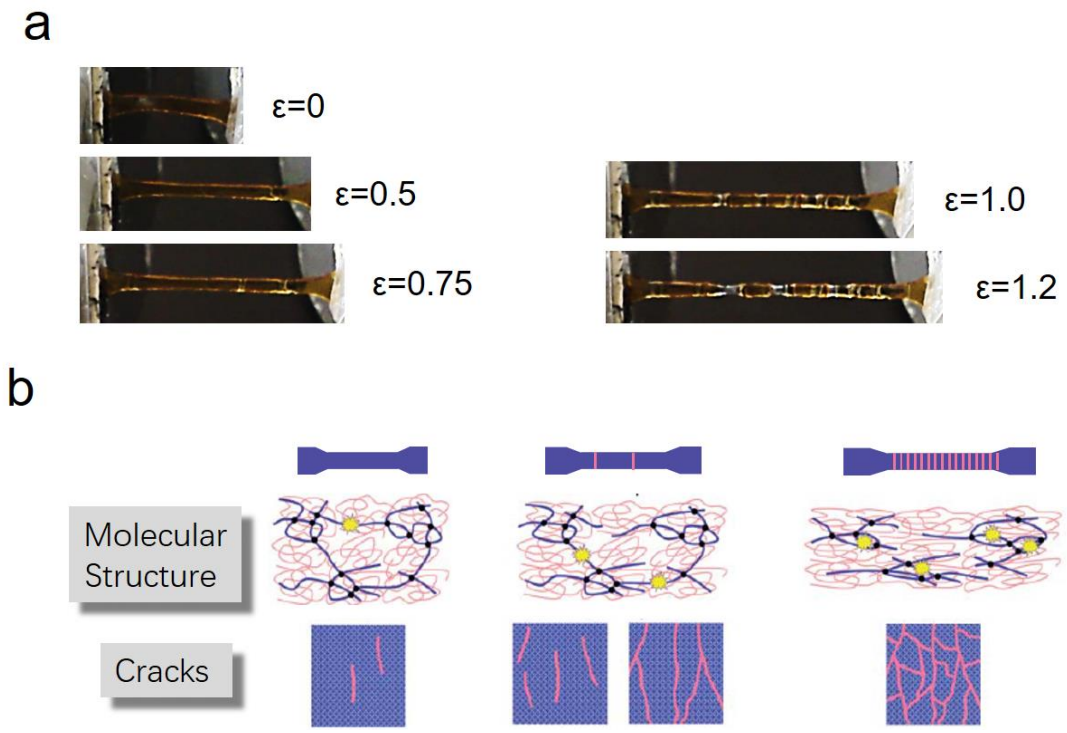


Figure 5.8 (a) Observation of fracture process and (b) scheme of sandwich P(HEA-*co*-AMA)/P(HEA-*co*-NBOC) composite hydrogels by UV irradiation on P(HEA-*co*-NBOC)-0.1.

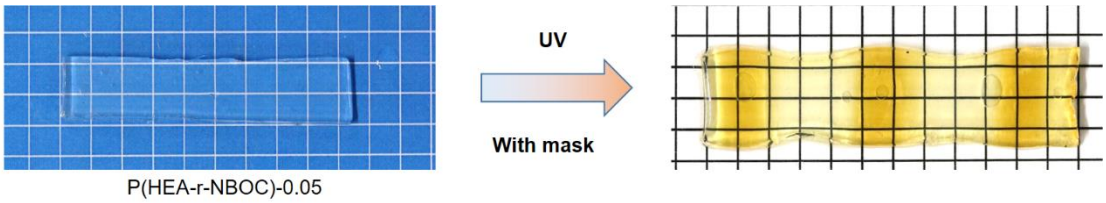


Figure 5.9 Deformation of 3D-patterned P(HEA-*co*-AMA)/P(HEA-*co*-NBOC) hydrogels by UV irradiation on P(HEA-*co*-NBOC)-0.05.

Chapter 6

Conclusion

In this dissertation, we provide a facile method to prepare hydrogel composites using photo-triggered local crosslinker transformation strategy, so that the gel consists of two modulus regions with molecular-level continuous interfaces and matched swelling ratio, which can be used as ideal macroscopic model for studying DN gels. The conclusions from each chapter are given as followed:

In the **chapter 3**, by addition of hydrophobic interaction between NBOC moieties into hydrophilic PUM networks, supramolecular hydrogels based on hydrophobic interaction and hydrogen bonds, acting as crossliners. This special combination of physical bonds results in high toughness, stiffness, fatigue resistance, and high mechanical performance. The reversible crosslikers, renders the self-recovery of the materials. The effect of fraction of NBOC and total monomer concentration on physical and mechanical properties of hydrogels were investigated and optimized. Since the NBOC monomer has multiple stimuli-response, integrating the stimuli-response into the tough hydrogel could be conducted in further studies. Therefore, these gels might open new avenue of tough hydrogels.

In the **chapter 4**, based on the addition of hydrophobic interaction by copolymerization

with NBOC, mechanical properties, toughness and fatigue resistance of P(UM-*co*-NBOC) hydrogels improved dramatically. Upon UV irradiation, part of physical crosslinkers composed of hydrophobic interaction transformed into chemical crosslinkers, which further enhance the mechanical properties. By control the UV irradiation depth and position, hybrid hydrogel consisted of different modulus regions can be easily prepared. This work provides a new strategy to fabrication tough hydrogel composites by incorporating a photo-responsive hydrophobic residue into the hydrogel network.

In the **chapter 5**, Based on addition of hydrophobic interaction by copolymerization with NBOC, mechanical properties, toughness and fatigue resistance of P(HEA-*co*-NBOC) hydrogels improved dramatically. After UV irradiation, part of physical crosslinkers composed of hydrophobic interaction transformed into chemical crosslinkers, new surface generated with instinctive mechanical properties. The hydrogels upon UV irradiation showed different Young's modulus. Thus, composite hydrogels based on copolymerization of photo-responsive, NBOC, and hydrophilic monomers, could be easily prepared *in situ* by UV irradiation. And their structure and properties could be modulated by thickness, f_{NBOC} and duration of UV irradiation.

List of Publications

Original papers

(1) **Zhen Tao**, Hailong Fan, Junchao Huang, Taolin Sun, Takayuki Kurokawa, and Jian Ping Gong, Fabrication of tough hydrogels composites from photo-responsive polymers to show double network effect, ACS Applied Materials and Interface, 11(40), 37139-37146 (2019).

(2) Hailong Fan, Jiahui Wang, **Zhen Tao**, Junchao Huang, Ping Rao and Jian Ping Gong, Adjacent cationic–aromatic sequences yield strong electrostatic adhesion of hydrogels in seawater, *accepted.*

Publications in Scientific Conferences

(1) **Zhen Tao**, Liang Chen, Kunpeng Cui, Honglei Guo, Hui Guo, Taolin Sun, Daniel R. King, Takayuki Kurokawa, Jian Ping Gong, Spatial control of noncovalent and covalent bond crosslink density on the mechanical strength of hydrogels, Hokkaido University-Impact Joint Symposium (08/2017, Sapporo, Japan)

(2) **Zhen Tao**, Hailong Fan, Junchao Huang, Kunpeng Cui, Taolin Sun, Takayuki Kurokawa, Jian Ping Gong, One-step fabrication of hydrogel composites with rigid surface, 67th SPSJ Symposium on Macromolecules (09/2018, Sapporo, Japan)

Acknowledge

The work of dissertation was performed under the direction of Professor Jian Ping Gong, from 2016 to 2019, at Hokkaido University, Japan.

Firstly, I would like to express my deepest gratitude and appreciation to my supervisor, Professor Jian Ping Gong, for her valuable advices, infinite patience, kind encouragement and excellent guidance during my doctoral course study. Her enthusiasm and rigorous attitude toward science strongly affected me and will continue to do so with my study and career in the future.

I also would like to express sincere gratitude to Professor Takayuki Kurokawa, Associate Professor Tasuku Nagajima, Assistant Professor Takayuki Nonoyama, Assistant Professor Daniel R. King, and Assistant Professor Kunpeng Cui, for their valuable discussions, helpful suggestions and helps to my study. I also want to thank Dr. Taolin Sun, our former lab member, who gave me illuminating instruction about my investigation and helped me a lot in my daily life.

I would like to thank Ms. Eiko Hasegawa, Miss Yuki Okubo, Ms. Ayako Kato, Ms. Yukiko Hane and Dr. Yoshinori Katsuyama for their kind paperwork supports and experimental supports.

I am also very thankful to all members in LSW, including Yiwan Huang, Ping Rao, Honglei Guo, Hui Guo, Yanan Ye, Liang Chen, Xueyu Li, Hailong Fan, Junchao Huang, Wei Cui, Yunzhou Guo, Chengtao Yu, Yong Zheng, Yang Han, Qifeng Mu, Jiahui Wang, Chenxi Yu, Yirong Cai, Dr. Tsutomu Indei, Ken-ichi Hoshino, Yuki Shibata, Takahiro Matsuda, Satoshi Hirayama, Takuya Kuriyama, Riku Takahashi, Martin Frauenlob, Kumi Ota, Yuhei Ozaki, Kazuki Fukao, Taiki Fukuda, Kei Mito, Joji Murai, Takuma Ikai, Akane Inoue, Yuto Uehara, Mai Kato, Runa Kawakami, Yong Woo Lee, Tsuyoshi Okumura, Kazuki Tanaka, Ryo Nanba, Kohei Murakawa, Ye Zhang, Masaya Iwata, Yumeko Kudo, Yuki Suzuki, Yukiko Takahashi, Kensuke Nakajima, Keigo Fujioka, Naoto Horihata, Chika Imaoka, Naohiro Kashimura, Takuya Nishimura, Koutaro Hata, Fumiya Muto, Tomoko Yamazaki, Taku Yokoyama, Hinako Kato, Ryotaro Nakamura, Shotaro Namiki, Masahiro Yoshida and Dr. Anaïs Giustiniani. They are always helping me with great kindness when I have problems in experiment.

I also would like to thank Takanori Sato, the landlord of my renting apartment, who provided me with great convenience and helped me a lot in my daily life. I also would like to express sincere gratitude to my friends in Japan, including Zhu Yuan, Xiao You, Li Peng, Qingge Lv and Baoxiang Li, with whose company, I spent joyful three years here.

I would like to dedicate this thesis work to my parents and other family members who have not only given me financial support, but also continuously provided me with love and patience. Special thanks to my beloved fiance, Renyi Zhou for always being with me, taking care of me, listening to me and giving me encouragement, especially during writing and editing my manuscript. I'm so grateful you came into my life. I would also thanks to my friends in China, who always give me supports and comfort.

This research was supported by JSPS KAKENHI Grant Numbers JP17H06144. The Institute for Chemical Reaction Design and Discovery (ICReDD) was established by World Premier International Research Initiative (WPI), MEXT, Japan.

Zhen Tao

March 2020 at Sapporo, Japan